African Journal of Biotechnology

Volume 16 Number 41, 11 October, 2017
ISSN 1684-5315

Academic Journals

ABOUT AJB

The African Journal of Biotechnology (AJB) (ISSN 1684-5315) is published weekly (one volume per year) by Academic Journals.

African Journal of Biotechnology (AJB), a new broad-based journal, is an open access journal that was founded on two key tenets: To publish the most exciting research in all areas of applied biochemistry, industrial microbiology, molecular biology, genomics and proteomics, food and agricultural technologies, and metabolic engineering. Secondly, to provide the most rapid turn-around time possible for reviewing and publishing, and to disseminate the articles freely for teaching and reference purposes. All articles published in AJB are peer-reviewed.

Contact Us

Editorial Office: ajb@academicjournals.org

Help Desk: helpdesk@academicjournals.org

Website: http://www.academicjournals.org/journal/AJB

Submit manuscript online http://ms.academicjournals.me/

Editorial Board

African Journal of Biotechnology

Table of Content: Volume 16 Number 41 11 October, 2017

ARTICLES

academicJournals

Vol. 16(41), pp. 1990-1996, 11 October, 2017
DOI: 10.5897/AJB2017.16212
Article Number: 61095B666257
ISSN 1684-5315

http://www.academicjournals.org/AJB

African Journal of Biotechnology

Full Length Research Paper

Evaluation of genetic diversity in rice (*Oryza sativa* and *Oryza glaberrima*) germplasm from Liberia and Ghana using simple sequence repeat (SSR) markers

Zogbo Luther[1,2*], Richard Akromah[2], Daniel Nyadanu[2], David P. Tokpah[1], Zipporah Page[1], Victor M. Voor[1] and Agnes D. Kwaloe[1]

[1]Central Agricultural Research Institute, Suakoko, Bong County, Liberia.
[2]Department of Crop and Soil Sciences, Faculty of Agriculture, Kwame Nkrumah University of Science and Technology, Kumasi, Ghana.

Received 17 August, 2017; Accepted 18 September, 2017

Rice is an important staple food crop that feeds over half of the global population and it has become the cereal that provides a major source of calories for the urban and rural poor in Africa. This research aimed to use simple sequence repeat (SSR) markers to evaluate the genetic diversity in rice (*Oryza sativa* and *Oryza glaberrima*) germplasm as breeding method. In the present study, 16 SSR markers were used across 48 genotypes or accessions obtained from Central Agricultural Research Institute (CARI), Suakoko, Liberia and Plant Genetic Resources Research Institute (PGRRI), Bunso, Ghana. DNA was extracted from 48 plants per accession without bulking to check the purity of the accession using the 16 SSR markers. Sixteen primers were acquired out of 20 primers which showed DNA amplification and polymorphism among the 48 rice accessions. The numbers of alleles detected by these 16 primers ranged from 1 to 16 with a mean of 5.25, while polymorphism information content (PIC) ranged from 0.06 to 0.66 with a mean of 0.35. The SSR markers were highly informative as generated by the power marker V3.25 software. The unweight pair group method with arithmetic averages (UPGMA) cluster dendrogram generated based on the 16 SSR markers grouped the accessions into 11 main clusters. At the similarity coefficients of 90%, the highly distance genetic diversity was found between 2 accessions; ACSS37 and ACSS1. Cluster X was the largest of all the clusters, while clusters VII and VIII were the second largest clusters with 7 accessions each. The outcome of this study should be useful to manage the gremplasm conservation and future rice genetic improvement.

Key words: Germplasm, genetic diversity, molecular markers, polymorphism, sequence repeat.

INTRODUCTION

Rice (*Oryza sativa* 2n = 24), and a member of Poaceae family (Gramineae) is the world's most important staple food crop that feeds over half of the global population, and it is cultivated in tropical and subtropical regions

*Corresponding author. E-mail: zobo.luther@yahoo.com. Tel: + 231+886-462-538.

(Khush et al., 2005). Rice is grown in more than 114 countries, over an area of 161.4 m ha in a wide range of ecosystems, under varying temperature and water regimes, with the production of 466.7 mt (on milled basis) (Yousaf et al., 2016). According to Sanni et al. (2013), approximately 20 million farmers are engaged in rice production in sub-Sahara Africa (SSA) and about 100 million people depend on it directly for their livelihoods in the continent.

Rice is rapidly becoming a staple food in the African diet; and its production in sub-Sahara Africa (SSA) continues to be outplaced by consumption because of low and stagnated production. Imported rice accounts for 50% of sub-Saharan Africa's rice requirement (Lee et al., 2010). Rice is no longer a luxury food but has become the cereal that constitutes a major source of calories for the urban and rural poor. Rice production in SSA has been bedeviled with conditions such as environmental degradation due to pesticide usage, excessive water usage, and nutrient contamination, methane emission and ammonia volatilization and all these conditions require urgent attention (Lee et al., 2010).

A wide range of technologies are available and can be used as tools for reducing these adverse consequences of rice production but they are, however, not extended to majority of rice growers or farmers (FAO/WHO, 2010). Rice production demand increases and little attention has been paid to the improvement of Liberian and Ghanaian rice germplasm evaluation and the genetics of some quality traits. Thus, there is very little information available on the genetic diversity of Liberian and Ghanaian rice germplasm for crop improvement and conservation purposes. Referencing an urgent need to increase and improve the production of rice in Africa in order to meet up with the high demand is necessary. The need for increasing rice cultivation depends not only on cultural/traditional practices, but also on their inbuilt genetic potential to withstand stresses. A successful breeding program will depend on the genetic variability for achieving the goals of improving the crop and producing high yielding varieties (Badiane et al., 2012). The first step in achieving this is to evaluate and characterize available rice germplasm or genotypes at molecular level; as genotypic diversity will reveal important traits or accessions of interest to plant breeders (Sugihara, 2017).

MATERIALS AND METHODS

Rice and their culture

The experiment was organized to study the genetic diversity of 52 rice accessions from Liberia and Ghana using SSR markers (Table 1). Two grams of young, fresh and healthy rice leaves were sampled, cleaned with 70% ethanol and placed in 2 ml Eppendorf using the cetyltrimethylammonium bromide (CTAB) method described by Earl (2010). In addition, samples were stored at 4°C until use.

Molecular markers and polymerase chain reactions

Sixteen simple sequence repeat markers (SSR) covering 20 chromosomes of rice were used to detect polymorphism among the rice accessions (Table 2). The SSRs markers were procured from Metabion International AG (Germany). Polymerase chain reaction (PCR) was carried out in Techne prime thermal cycler (Labnet International Inc., California, USA) and GeneAmp PCR System 9700 (Applied Biosystems, USA) of 96-well plates with heated lid to reduce evaporation. The DNA from the 48-tagged rice samples were fingerprinted using SSR markers. Nine µl of premix of 3.3 µl double distilled water, 5.0 µl buffer + dNTPs (deoxynucleotide triphosphates), 0.02 µl $MgCl_2$, 0.6 µl forward and reverse primers and 0.08 µl Taq polymerase was pipetted into 200 µl tube. After that 1 µl of 4 ng/µl DNA was added to make a total volume of 10 µl. The reaction mixtures were short spun and placed in the thermal cycler and ran with the following program: 3 min at 94°C followed by 30 s at 94°C for denaturing, 30 s at 55°C for annealing, 1 min at 72°C for extension, repeated for 35 cycles, and final extension of 7.0 min at 72°C amplified samples were held at 4°C.

Gel electrophoresis

The PCR products were separated using horizontal agarose gel electrophoresis. The amplified DNA fragments were separated on 2.0 % agarose gel stained with 0.005% gel-red solution. After that, 2 µl loading dye (6X Bromophnol blue) was added to the PCR products. The gel was set, the PCR products were added in wells submerged in 1× TBE buffer. The samples were then run at 120 volts for 2 h, observed on the UV transilluminatar and photographed.

Bands of DNA scoring

The qualitative points from the amplified polymorphic products were scored as (0) which indicates no symptoms and (1) which indicates symptoms for each marker allele-genotype combination, and the markers were calculated using Power Marker V3.25 computer software.

SSR data analysis

A sequential agglomerative and hierarchical clustering dendrogram which illustrates the genetic relationship among the rice genotypes, was constructed using weighted pair group method with arithmetic mean (UPGMA) algorithm for clustering and simple matching (SM) similarity coefficient in NTSYS software (2.2). Sequential and hierarchical nested (SAHN) option was employed (Klingenberg et al., 2010). Gene diversity, allele frequency, number of alleles, heterozygosis and polymorphic information content (PIC) values of the markers were calculated using Power Marker V3.25 computer software.

RESULTS

Sixteen SSR loci were evaluated for their efficiency of polymorphism against 48 accessions of rice received from 2 countries. Among the 20 SSR primers used in this study, 16 yielded scorable amplification products (Table 3). Major allele frequency revealed by the markers across the 48 rice accessions ranged from 0.50 Rm474 (11) to 0.97 RM43 (15), with a mean of 0.76. The number of

Table 1. Accessions of rice's, their sources and collection countries.

Accession number	Name	Source	Accession number	Name	Source
1	LAC 23-1	AFRICA RICE / LIBERIA	25	GH 1536	PGRRI/GHANA
2	LAC 23-2-2	AFRICA RICE / LIBERIA	27	GH 1594	PGRRI/GHANA
3	LAC 23-2-3	AFRICA RICE / LIBERIA	28	GH 2144	PGRRI/GHANA
4	LAC 23-3	AFRICA RICE / LIBERIA	29	GH 1593	PGRRI/GHANA
5	LAC 23-4	AFRICA RICE / LIBERIA	31	GH1588	PGRRI/GHANA
6	LAC 23-5	AFRICA RICE / LIBERIA	32	GH 1587	PGRRI/GHANA
7	LAC 23-6	AFRICA RICE / LIBERIA	33	GH 1580	PGRRI/GHANA
8	LAC 23-7	AFRICA RICE / LIBERIA	34	GH1581	PGRRI/GHANA
9	LAC 23-8	AFRICA RICE / LIBERIA	35	GH 1578	PGRRI/GHANA
10	LAC 23-9	AFRICA RICE / LIBERIA	36	GH 1575	PGRRI/GHANA
11	LAC 23-10	AFRICA RICE / LIBERIA	37	GH 1572	PGRRI/GHANA
12	LAC 23-11	AFRICA RICE / LIBERIA	38	GH 1579	PGRRI/GHANA
13	LAC 23-12	AFRICA RICE / LIBERIA	39	GH 1584	PGRRI/GHANA
14	GH 1510	PGRRI/GHANA	40	GH 3623	PGRRI/GHANA
15	GH 1515	PGRRI/GHANA	41	GH 1576	PGRRI/GHANA
16	GH 1518	PGRRI/GHANA	42	GH 1550	PGRRI/GHANA
17	GH 2204	PGRRI/GHANA	43	GH 1598	PGRRI/GHANA
18	GH 2193	PGRRI/GHANA	44	GH 1570	PGRRI/GHANA
19	GH 1512	PGRRI/GHANA	47	GH 1573	PGRRI/GHANA
20	GH 1521	PGRRI/GHANA	48	GH 1523	PGRRI/GHANA
21	GH 1534	PGRRI/GHANA	49	GH 1549	PGRRI/GHANA
22	GH 1538	PGRRI/GHANA	50	GH 1524	PGRRI/GHANA
23	GH 1526	PGRRI/GHANA	51	GH 1540	PGRRI/GHANA
24	GH 1528	PGRRI/GHANA	52	GH 1571	PGRRI/GHANA

Table 2. List of rice SSR markers used in the DNA fingerprinting.

S/N	Marker name	Primers sequence (5'- 3')	Number of bases	Motif	Number of repeats	Chromosomes	Amplified product size
1	RM 105-F RM105-R	GTCGTCGAC CCA TCG GAG CCAC TGGTCG AGGTGG GGA TCG GGT C	22 22	CCT	6	9	134
2	RM 125-F RM 125-R	ATCAGCAGCCATGGCAGCGACC AGGGGATCATGTGCCGAAGGCC	22 22	GCT	8	7	127
3	RM 11-F RM 11-R	TCTCCTCTTCCCCCGATC ATAGCGGGCGAGGCTTAG	18 18	GA	17	7	140
4	RM 25-F RM 25-R	GGAAAGAATGATCTTTTCATGG CTACCATCAAAACCAATGTTC	22 21	GA	18	8	146
5	RM 408-F RM 408 -R	CAACGAGCTAACTTCCGTCC ACTGCTACTTGGGTAGTCGACC	20 22	CT	13	8	128
6	RM 536-F RM 534-R	TCTCTCCTCTTGTTTGGCTC ACACACCAACACGACCACAC	20 20	CT	16	11	243
7	RM 552-F RM 552-R	CGCAGTTGTGGATTTCAGTG TGCTCAACGTTTGACTGTCC	20 20	TAT	13	11	195
8	RM 484-F RM 484-R	TCTCCCTCCTCACCATTGTC TGCTGCCCTCTCTCTTCTTC	20 20	AT	9	10	299

Table 2. Contd.

9	RM 171-F RM 171-R	AACGCGAGGACACGTACTTAC ACGAGATACGCTCGCCTTTG	21 20	GATG	5	10	328
10	RM 271-F RM 271-R	TCAGATCTACAATTCCATCC TCGGTG AGACCTAGAGAGCC	21 20	GA	15	10	101
11	RM 474-F RM 474-R	AAGATGTACGGGTGGCATTC TATGAGCTGGTGAGCAATGG	20 20	AT	13	10	252
12	RM 215-F RM 215-R	CAAAATGGAGCAGCAAGAGC TGAGCACCTCCTTCTCTGTAG	20 21	CT	16	9	148
13	RM316-F RM 316-R	CTAGTTGGGCATACGATGGC ACGCTTATATGTTACGTCAAC	20 21	GT	8	9	192
14	RM 447-F RM 44-R	CCCTTGTGCTGTCTCCTCTC ACGGGCTTCTTCTCCTTCTC	20 20	CTT	8	8	111
15	RM 433-F RM 433-R	TGCGCTGAACTAAACACAGC AGACAAACCTGGCCATTCAC	20 20	AG	13	8	224
16	RM118-F RM 118-R	CCAATCGGAGCCACCGGAGAGC CACATCCTCCAGCGACGCCGAG	22 22	GA	8	7	156

F=forward primer; R=Reverse primer. Source: Metabion International Laboratory, Germany.

Table 3. Summary statistics of the16 SSR Markers.

Marker	Allele frequency	Allele number	Gene diversity	Heterozygosity	PIC
RM105(SSR1)	0.84	7.00	0.28	0.32	0.27
RM125(SSR1)	0.70	6.00	0.49	0.52	0.47
RM11(SSR3)	0.66	7.00	0.54	0.69	0.52
RM25 (SSR4)	0.92	4.00	0.16	0.17	0.15
RM408(SSR5)	0.57	6.00	0.63	0.87	0.59
RM536(SSR6)	0.88	5.00	0.23	0.25	0.22
RM552(SSR7)	0.56	5.00	0.58	0.87	0.51
RM484(SSR8)	0.50	7.00	0.68	0.98	0.65
RM171(SSR9)	0.63	6.00	0.55	0.74	0.50
RM271(SSR10)	0.92	6.00	0.16	0.12	0.16
RM474(SSR11)	0.50	10.00	0.69	1.00	0.66
RM215(SSR12)	0.75	3.00	0.38	0.50	0.33
RM316(SSR13)	0.89	3.00	0.20	0.22	0.19
RM447(SSR14)	0.95	3.00	0.10	0.11	0.10
RM43 (SSR15)	0.97	3.00	0.06	0.06	0.06
RM118(SSR16)	0.92	3.00	0.16	0.17	0.15
Mean	0.76	5.25	0.37	0.47	0.35

PIC, Polymorphic information content.

alleles per locus ranged from SSR Marker RM474, RM484, RM11, RM105, and RM125, recorded as the highest number of allele number detected (10.00, 7.00, 7.00, 7.00, 6.00) (Table 3). RM536 and RM 552 (5.00, 5.00) followed this in that order, the least were RM 215, RM 316, RM 447s, RM43 and RM 118, with the total

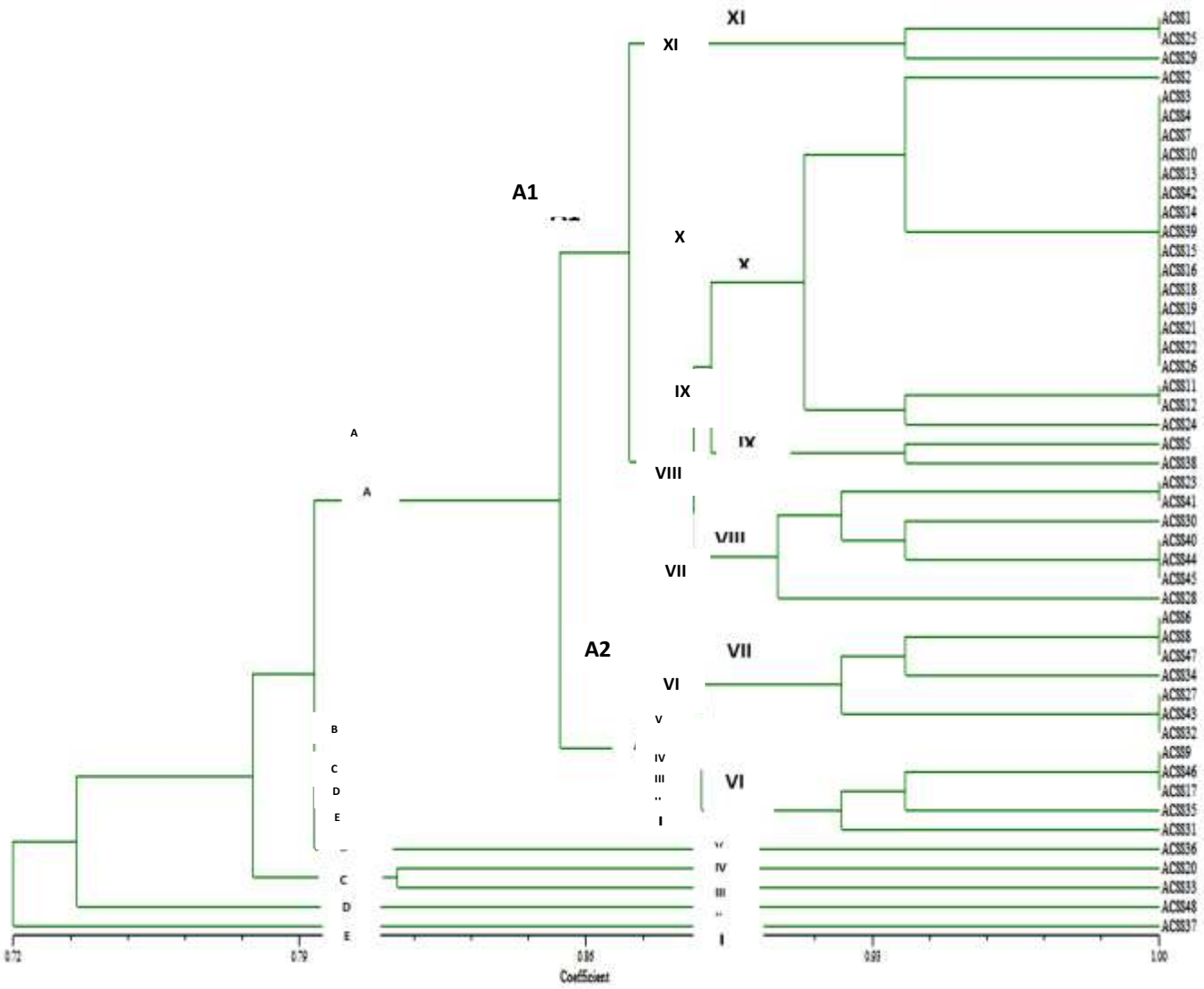

Figure 1. Dendrogram based on 16 SSR markers for 48 rice accessions using SM similarity coefficient and UPGMA clustering.

mean of 5.25. RM474 (11) had the highest heterozygosis of 1.00 followed by RM484 (8) 0.98 and RM552 (5) 0.87, with a scoring of 0.47 heterozygosis. While SSR markers RM43 (15) 0.06 and RM447 (14) 0.11 recorded the least heterozygosis with an average of 0.47 (Table 3). The mean PIC value for all markers used was 0.35 and ranged between 0.06 and 0.66 in loci RM43 (15) and RM474 (11), respectively. Gene diversity ranged from 0.06 in RM43 (15) to 0.69 in RM11 (3), with a mean of 0.37. Generally, the allele frequency of all the markers was below 0.95, indicating that they were all polymorphic in character (Table 3).

Genetic relationship revealed by the six 16 primers using similarity coefficients based on unweight pair group method with arithmetic means (UPGMA) is shown in Figure 1. From the figure, a dendrogram was constructed to ascertain the genetic diversity and relatedness among 48 rice genotypes. The dendrogram indicated similarity values ranging from 1.00 to 0.72, with 11 main clusters: I, II, III, IV, V, VI, VII, VIII, IX, X and XI at similarity coefficients of 90%. The highest genetic distance was found between accessions; ACSS37 from Ghana and ACSS1 from Liberia. These accessions took the first and last positions of the dendrogram, respectively. Cluster X was the largest of all the clusters and it contained 19 accessions, 13 of the accessions were from Liberia while 6 came from Ghana, with 4 sub-clusters. Clusters VII and VIII were the second largest clusters with 7 accessions each. Cluster VII had 3 sub-clusters, while cluster VIII comprised of 4 sub-clusters. Clusters I to V contained 1 accession each, and cluster VI had 5 accessions with 3 sub-clusters. Cluster IX comprised of 2 accessions and was sub divided into 2 sub-clusters. The accessions 17, 9, 47, 8, 6, 44, 40, 26, 22, 21, 19, 18, 39, 15, 14, 42, 13,

10, 7, 4, 3 and 2 that came from both Ghana and Liberia were very similar at 100% similarity coefficient.

DISCUSSION

Plant breeders referenced information on genetic diversity and relatedness in crop germplasm because it assists them in planning crosses (Chakhonkaen et al., 2012). This information is useful in designing strategies used to improve traits, maintain and manage germplasm in Genetic Resource Centres, or enhance the genetic base of future varieties. Hence, to effectively maintain, evaluate and utilize germplasm, it is important to investigate the extent of available diversity. In the present work, a set of rice genotypes were subjected to diversity analysis based on variation in SSR molecular profiles.

Twenty SSR markers were collected from two countries, with their genetic variability characterized and assessed among 48 rice accessions. Sixteen out of these 20 SSR markers revealed genetic polymorphism and ensured unambiguous identification of the rice accessions. Small numbers of molecular markers were used to assess genetic diversity as shown earlier in other studies.

Sixteen SSR primers yielded 84 alleles ranging from RM105 (1) to RM118 (16), with an average of 5.25 alleles per locus and were similar to those earlier reported by Chen et al. (2002). They used Indian quality rice germplasm and reported an average of 6.80 alleles per locus. The number of alleles detected in the present study is lower than those observed by Chakhonkaen et al. (2012), who reported 127 alleles that ranged from 4 to 12 alleles using 19 InDel (Insertion-Deletion) markers to evaluate genetic diversity in 101 rice accessions. In another study, Hossain et al. (2012) found an average of 3.8 alleles per locus in rice using Bangladeshi ARLs. The obtained results were also comparable to 2.0 to 5.5 alleles per SSR locus for various classes of microsatellites reported by Kong et al. (2000), who used a different set of rice germplasm. Wong et al. (2009) reported the genetic relationship and diversity analysis among 8 Bario rice cultivars using 12 SSR primers, detecting a total of 31 alleles. The average genetic diversity of 0.37 obtained was lower compared to 0.55 previously reported by Sajib et al. (2012), who used 9 SSR markers to study genetic diversity among 12 aromatic landraces of rice. Polymorphism information content (PIC) is a measure of polymorphism among varieties for a marker locus used in linkage analysis (Sajib et al., 2012). It ranged from 0.06 to 0.66, with an average of 0.35 in this study. The PIC range and average observed in this study are similar to those reported earlier by Meti et al. (2013); they reported PIC range of 0 to 0.74 with an average of 0.58 using 12 SSR markers to estimate genetic diversity in 48 aromatic rice genotypes merge. Higher values of PIC might be the result of diverse genotypes and lower values might be the result of closely related genotypes (Coldea et al., 2010).

The dendrogram showed that there were genetic variations among the 48 rice accessions in relation to the used SSR primers. The similarity coefficient of these accessions ranged from 0.72 to 1.00, which is an indication of the genetic variation among the accessions based on the SSR primers. The observed variation among the accessions is an indication that SSR markers can reveal diversity existing among rice accessions. This is in agreement with earlier findings of Meti et al. (2013); they reported that SSR markers are effective tools in differentiating rice genotypes. In some relevant research, classification methods based on genetic background were not been concerned well (Tokpah et al., 2017), which resulted in duplication of same species and time-consuming. The accessions were grouped into 11 main clusters at similarity coefficients of 90%. The highest genetic distance was found between the accessions; ACSS37 from Ghana and ACSS1 from Liberia. These accessions had the first and last positions of the dendrogram, respectively. In addition, at a similarity coefficient of 90%, cluster X was the largest of all the clusters and it contained 22 accessions with 4 sub-clusters. Cluster X sub-cluster 3 from Ghana and Liberia had 13 and 9 accessions which showed 100% similarity, revealing that no genetic variability exist among these accessions based on the 16 SSR primers. The similarity could have risen from informal exchange of seeds (germplasm) among farmers, but given different names because of the differences in dialect and ethnic groups. It is important to eliminate duplicates to enable effective management, conservation of germplasm and reduced workload for further experiment.

Conclusion

The present work helped in strengthening the background necessary for promoting and breeding of improved varieties of rice. At the molecular level, 48 rice accession from Ghana and Liberia were observed. Among the studied accessions, 18 out of the 48 accessions were distant from the rest and were selected to constitute a core collection for further improvement. In addition, broadening the genetic base of rice in breeding programs is urgently needed to enhance heterozygosis in crosses and create heterotic progenies. Overall, this study has explained the relevance of employing molecular markers to determine genetic distances and relationships in rice. Moderate level of genetic diversity was observed among the rice accessions.

CONFLICT OF INTERESTS

The authors have not declared any conflict of interests.

REFERENCES

Badiane FA, Gowda BS, Cissé N, Diouf D, Sadio O, Timko MP (2012). Genetic relationship of cowpea (*Vigna unguiculata*) varieties from Senegal based on SSR markers. Genet. Mol. Res. 11(1):292-304.

Chakhonkaen S, Pitnjam K, Saisuk W, Ukoskit K, Muangprom A(2012). Genetic structure of Thai rice and rice accessions obtained from the International Rice Research Institute. Rice 5(1):19.

Chen M, Presting G, Barbazuk WB, Goicoechea JL, Blackmon B, Fang G, Kim H, Frisch D, Yu Y, Sun S, Higingbottom S (2002). An integrated physical and genetic map of the rice genome. Plant Cell Online 14(3):537-545.

Coldea R, Tennant DA, Wheeler EM, Wawrzynska E, Prabhakaran D, Telling M, Habicht K, Smeibidl P, Kiefer K (2010). Quantum criticality in an Ising chain: experimental evidence for emergent E8 symmetry. Science 327(5962):177-180.

Earl DA (2012). Structure harvester: a website and program for visualizing structure output and implementing the Evanno method. Conserv. Genet. Resour. 4(2):359-361.

Food and Agriculture Organization/World Health Organization (FAO/WHO) (2010). Joint FAO/WHO Expert Committee on Food Additives. Meeting, and World Health Organization. Evaluation of Certain Food Additives: Seventy-first Report of the Joint FAO/WHO Expert Committee on Food Additives. World Health Organization. Vol. 71.

Hossain MA, Piyatida P, da Silva JA, Fujita M (2012). Molecular mechanism of heavy metal toxicity and tolerance in plants: central role of glutathione in detoxification of reactive oxygen species and methylglyoxal and in heavy metal chelation. J. Bot. 2012 Apr 2; 2012.

Klingenberg CP (2010). Evolution and development of shape: integrating quantitative approaches. Nat. Rev. Genet. 11(9):623.

Kong J, Franklin NR, Zhou C, Chapline MG, Peng S, Cho K, Dai H (2000). Nanotube molecular wires as chemical sensors. Science 287(5453):622-625.

Lee HM, Baines MJ, Mattia A, Knaap A(2010). sucrose oligoesters Type I and Type II." Safety evaluation of certain food additives, P 249.

Meti N, Samal KC, Bastia DN, Rout GR (2013). Genetic diversity analysis in aromatic rice genotypes using microsatellite based simple sequence repeats (SSR) marker. Afr. J. Biotechnol. 12(27): 4238-4250.

Sajib AM, Hossain M, Mosnaz AT, Hossain H, Islam M, Ali M, Prodhan SH (2012). SSR marker-based molecular characterization and genetic diversity analysis of aromatic landreces of rice (*Oryza sativa* L.). J. BioSci. Biotechnol. 1(2):107-116.

Sanni KA, Touré AA, Diagne A, Bachabi F, Murori R, Singh RK, Sié M (2013). 6 Rice Varietal Release Systems in Africa. Realizing Africa's rice promise. CAB International, Wallingford. pp. 79-86.

Sugihara S (2017). Utilization of Soil Microbes as a Temporal Nutrient Pool to Synchronize Nutrient Supply and Uptake: A Trial in the Dry Tropical Croplands of Tanzania. In. Soils, Ecosystem Processes, and Agricultural Development. Springer Japan. pp. 357-379.

Tokpah DP, Li H, Newmah JT, Page Z, Luther Z, King CF, Smith MS, Voor VM (2017). Biological control of potential antagonistic bacteria isolates to restrict Magnaporthe grisea infection on rice. Afr. J. Microbiol. Res. 11(27):1108-1119.

academicJournals

Vol. 16(41), pp. 1997-2008, 11 October, 2017
DOI: 10.5897/AJB2017.16214
Article Number: 48C7FC366259
ISSN 1684-5315

http://www.academicjournals.org/AJB

African Journal of Biotechnology

Full Length Research Paper

Xylose recovery from dilute-acid hydrolysis of oil palm (*Elaeis guineensis*) empty fruit bunches for xylitol production

Katherine Manjarres-Pinzón[1*], Mario Arias-Zabala[1], Guillermo Correa-Londoño[2], and Eduardo Rodriguez-Sandoval[3]

[1]Escuela de Química, Facultad de Ciencias, Universidad Nacional de Colombia-Medellín, Antioquia, Colombia.
[2]Departamento de Ingeniería Agronómica, Facultad de Ciencias Agrarias, Universidad Nacional de Colombia – Medellín, Antioquia, Colombia.
[3]Departamento de Ingeniería Agrícola y Alimentos, Facultad de Ciencias Agrarias, Universidad Nacional de Colombia-Medellín, Antioquia, Colombia.

Received 18 August, 2017; Accepted 28 September, 2017

The aim of this study was to evaluate the effect of different process conditions, such as the sulfuric acid concentration, contact time, solid:liquid ratio and particle size, on the xylose recovery and the formation of by-products from oil palm empty fruit bunch (OPEFB) with dilute-acid hydrolysis. Moreover, an adapted and non-adapted strain of the yeast *Candida guilliermondii* was used to obtain xylitol from the optimal hydrolysate. Xylose, glucose, hydroxymethylfurfural (HMF) and acetic acid in the acid hydrolysate were analyzed with high performance liquid chromatography (HPLC). A Box-Behnken-based design was used to find the combination of factors that maximized the formation of xylose in the hydrolysate optimization process. The fermentation to obtain xylitol from the optimized hydrolysate of OPEFB with adapted and non-adapted *C. guilliermondii* strains was made in 100 ml Erlenmeyer flasks at 30°C for 96 h at 200 rpm in an incubator shaker. The maximum xylose concentration (32.59 g L^{-1}) was obtained at 121°C, for 30 min, with a 1:8 solid:liquid ratio, 2% acid concentration and particle size of around 4 cm. With the same conditions, the inhibitor concentrations, such as HMF, glucose and acetic acid, were 0.023, 1.033 and 11.078 g L^{-1}, respectively. The optimized conditions were the same as previously described. The higher xylitol productivity (10.3 g L^{-1}) and yield (0.43 g g^{-1}) were obtained by fermentation with non-adapted *C. guilliermondii* strains from the optimized hydrolysate of OPEFB without the need for detoxification. It is not necessary to make an adaptation of *C. guilliermondii* in the optimized hydrolysate of OPEFB to produce xylitol.

Key words: Oil palm, empty fruit bunches, xylose, dilute-acid hydrolysis, xylitol.

INTRODUCTION

Oil palm (*Elaeis guineensis* Jacq.*)* is the highest yielding edible oil crop in the world. It is cultivated in 42 countries, with 11 million ha worldwide. Colombia is the largest producer of oil palm in Latin America and the fourth largest producer in the world (Fedepalma, 2014). Oil palm empty fruit bunches (OPEFB) constitute 21% of the total weight of harvested fruits. OPEFB fiber is one of the most promising significant resources of biomass waste

and it is produced from the oil palm extraction of fresh fruit bunches. This biomass is a rigid cellulose structure combined with an amorphous hemicellulose and lignin cross-linked structure and is usually burned in incinerators by oil palm mills, which creates environmental pollution problems in the neighboring areas (Kim and Kim, 2013). The OPEFB biomass contains 42.7% cellulose, 17.1% hemicellulose and 13.2% lignin (Hassan et al., 2013).

Moreover, OPEFB contain 24% xylan, a sugar polymer made up of pentose sugar xylose, which can be used as a substrate for the production of different compounds with chemical and biochemical processes (Rahman et al., 2007). Xylan is the most abundant polysaccharide in hemicelluloses and is more susceptible to hydrolysis by mild acid treatments due to its amorphous structure, as compared to cellulose, which needs severe treatment conditions because of its crystalline nature (Shatalov and Pereira, 2012). Although xylose was the main sugar obtained from the hemicellulose, other by-products, such as glucose, acetic acid and furfural, were also produced in low amounts during the hydrolysis process (Dominguez et al., 1997; Silva et al., 1998; Rahman et al., 2007).

Acetic acid and furfural are considered potential inhibitors to yeast metabolism by causing cell morphological change or ultimate death of the organism. Further, high glucose concentration can repress the xylose reductase activity, which is involved in the conversion of xylose to xylitol (Mardawati et al., 2015). Thus, the concentration of these by-products should be kept at a low level to run the hydrolysis reaction at less severe conditions. The pretreatment of lignocellulose to obtain fermentable sugars is an essential step for lignocellulose conversion with microbial fermentation. A variety of pretreatment methods using mechanical, chemical and biological processing have been developed to change the structural and chemical composition of lignocellulose in order to improve sugar yields (Carvalho et al., 2013; Duangwang and Sangwichien, 2013; Liu and Wang, 2016). Among these methods, an acid hydrolysis pretreatment can be done with concentrated or diluted-acid, but the use of concentrated acids is less desirable because inhibitory compounds are formed. Furthermore, concentrated acid pretreatment methods generate more problems with equipment corrosion and acid recovery (Rocha et al., 2014). It has been recommended to use an acid concentration of about 1% (w/v) for optimal xylose yields (Zhang et al., 2012). Dilute-acid hydrolysis is probably the most commonly applied and frequently investigated method among the chemical pretreatment methods that are used. The main objectives of the acid hydrolysis pretreatment stage are to solubilize the hemicellulosic fraction of the biomass and to increase the accessibility of the cellulose to the enzymes (Zhang et al., 2012; Rocha et al., 2014).

The dilute-acid hydrolysis process usually uses sulphuric acid and hydrochloric acid at concentrations of 1 to 10% at a moderate temperature (in the range of 100 to 150°C) and produces an aqueous fraction containing mainly hemicellulosic sugars (Lenihan et al., 2010). These sugars consist of monosaccharides (xylose, glucose, arabinose) and xylo-oligosacharides (Alfaro et al., 2009; Yañez et al., 2009), which can be further hydrolyzed and fermented to obtain several products like xylitol (Ferrer et al., 2013).

Xylitol, a naturally occurring five-carbon sugar alcohol, has applications in the pharmaceutical, food, and odontological industries owing to its similar high sweetening power, but fewer calories, relative to sucrose. However, current commercial xylitol production processes require high-pressure conditions (up to 50 atm), as well as the toxic nickel catalyst, rendering the chemical process expensive and environmentally unfriendly (Hong et al., 2016). The alternative biotechnological production of xylitol from hemicellulosic hydrolysates and industrial by-products has been proposed, since the process is relatively easy and the cost of production is cheaper than that with chemical methods. The yields of xylitol correspond to only 50 to 60% of xylan present in the raw materials. Among the microorganisms that can assimilate xylose, yeasts belonging to the genus *Candida* sp. are the best xylitol producers (Miura et al., 2015).

In general to produce value-added compounds such as ethanol, xylitol, etc., cells must cope with different conditions in industrial processes such as high concentration of inhibitory products, osmotic problems, high process temperatures, and growth conditions that are not well controlled (Tomás-Pejó et al., 2010). Evolutionary engineering or adaptive strategies are promising alternatives to develop more tolerant yeasts. Directed adaptation of yeast to inhibitory prehydrolysate is one interesting strategy to enhance the process efficiency (Tomás-Pejó et al., 2010). Several studies reported that adapted yeast strains, such as *Pichia kudriavzevii* and *Saccharomyces cerevisiae*, had higher ethanol production from sugarcane juice, wheat straw or sugarcane bagasse hydrolysates compared to the non-adapted strains (Martín et al., 2007; Tomás-Pejó et al., 2010; Dhaliwal et al., 2011). With regards to *C. guilliermondii*, the xylitol production from concentrated sugarcane bagasse and rice straw hemicellulosic hydrolysates was performed using adapted and non-adapted strains. The xylitol yield increased with the first strain, showing that the more adapted strains can

*Corresponding author. E-mail: jkmanjarresp@unal.edu.co. Tel: +57-4-4309072.

efficiently reduce xylose to xylitol in hemicellulose hydrolysates (Sene et al., 2001; Silva and Roberto, 2001).

This study aimed to evaluate the effect of the sulfuric acid concentration (2, 4 and 6% (w/v)); contact time (20, 30 and 40 min), solid:liquid ratio (1:8; 1:10 and 1:12) and particle size (0.5, 3 and 4 cm) on the release of xylose and the formation of by-products [glucose, acetic acid and hydroxymethylfurfural (HMF)] from the dilute-acid hydrolysis of OPEFB biomass. A Box-Behnken-based design was used to find the combination of factors that maximized the formation of xylose in the hydrolysate optimization process and to assess the influence of these treatments on the morphology and microstructure of OPEFB. Moreover, bioconversion of the optimal hydrolysate to xylitol by the yeast *C. guilliermondii* was investigated using an adapted and non-adapted strain.

MATERIALS AND METHODS

Raw material

The OPEFB (20 kg) were collected in August, 2015 from Palmar del Oriente S.A.S., a local oil palm mill located at 4.40073 latitude and 75.40819 longitude, in Villanueva, Casanare, Colombia. They were disinfected, oven-dried at 60°C for 24 h and ground using a blade mill. The milled OPEFB was sieved using a Ro-Tap (Model B, W.S. Tyler Inc., Gastonia, NC, USA), resulting in the separation of different particle sizes, between 0.05 and 4 cm. The milled and sieved OPEFB were packed in polyethylene bags and stored at 30°C and 60% relative humidity (RH). The moisture, ash, and cellulose, hemicellulose and lignin contents of the dried OPEFB were determined according to National Renewable Energy Laboratory protocols, NREL/TP 510-42621, NREL/TP 510-42622 and NREL/TP 510-42618, respectively (Sluiter et al., 2008, 2012).

OPEFB dilute-acid hydrolysis

The dilute-acid hydrolysis of the OPEFB biomass was carried out in 125 ml Erlenmeyer flasks at 121°C for 20, 30 and 40 min, with a solid/liquid ratio of 1:8; 1:10 and 1:12, an aqueous H_2SO_4 solution of 2, 4 and 6% (w/v) and particle size of 0.05, 3 and 4 cm. After the hydrolysis process, the Erlenmeyer flasks were quickly immersed in an ice water bath to stop the reaction. The solids were separated from the aqueous solution with filtration. The hydrolysate was analyzed for xylose, glucose, acetic acid and HMF (Roberto et al., 2003).

Xylitol production

The most effective treatment was chosen from the OPEFB dilute-acid hydrolysis. Then, two treatments with *C. guilliermondii* (ATCC 6260, Microbiologics®, St. Cloud, MN) inoculation were performed: adapted and non-adapted strains to the hydrolysate. The adapted strains were obtained by mean of successive inoculations in mediums with optimized hydrolysate component, as follows: a loop full of yeast was transferred to sterilized 100-ml Erlenmeyer flasks containing 20 ml of yeast extract, peptone and glucose (YPG) medium as the primary inoculation, which was incubated at 30°C for 48 h at 108 rpm in an incubator shaker. An aliquot of 2 ml was then inoculated into 100 ml Erlenmeyer flasks containing 18 ml of medium, YPG and the optimized hydrolysate of OPEFB, at the same incubation conditions. Sequential transferring of the inoculum (2 ml) was done as described previously for increasing concentrations of the optimized hydrolysate of OPEFB (20, 50, 70, and 100%), so that strains could adapt to the physiological conditions of the medium. Cell culture growth at potato/dextrose/agar (PDA) was monitored at each step during successive inoculation of strains until a significant increase in cell concentration was observed (Aguilera and Benitez, 1989; Oberoi et al., 2010).

The batch fermentation was performed in 100 ml Erlenmeyer flasks with 47 ml of the optimized hydrolysate of OPEFB at 30°C for 96 h at 200 rpm in an incubator shaker. The system pH of the medium was maintained at 5.5. The inoculum concentration (3 g L^{-1}) with yeast viability of 98% determined by Neubauer chamber (Saeed et al., 2010) and xylose concentration (40 g L^{-1}) were also kept constant in each fermentation batch. These flasks were inoculated separately with adapted and non-adapted *C. guilliermondii* strains, under sterile conditions. The parameters evaluated were xylitol concentration and product yield coefficient (Yp/s), which is the xylitol yield based on the xylose consumption (g of xylitol per g of xylose) (Manjarres-Pinzón et al., 2016). At least four repetitions for this process were carried out.

Analytical methods

Sugars and inhibitor concentrations

The xylose, glucose and HMF in the acid hydrolysate, and the xylitol in the fermentation process were analyzed with HPLC (Shimadzu Prominence 20A, Kyoto, Japan), using an Aminex HPX-87H (Biorad) column and RI detector. Aqueous H_2SO_4 (0.005 M) was used as the mobile phase with a flow rate of 0.6 ml/min. The oven temperature was maintained at 65°C. The injection volume was 20 µl, with an isocratic method (Piñeros-Castro et al., 2011). Moreover, the acetic acid was determined using the same HPLC and column, but with a UV detector and at room temperature. The detection wavelength of this acid was set at 203 nm. D(+)-xylose (142080.1208, Pancreac, Química SAU, Spain), D(+)-glucose anhydrous (141341.1211, Pancreac, USA), 5-hydroxymethyl-2-furaldehyde (CAS 67.47.0, Sigma-Aldrich, USA), acetic acid glacial (CAS 64.19.7, Scharlab S.L., Spain) and xylitol (CAS 87.99.0, Sigma-Aldrich, USA) were used as the internal standards (IS). The quantification was done by measuring the ratio of the peak area of the sample to that of the IS. Primary standard stock solutions of xylose, glucose, acetic acid, HMF and xylitol were prepared in aqueous H_2SO_4 at a concentration of 0.005 M.

Morphological changes of OPEFB

Scanning electron microscopy (SEM)

The morphology and changes in the physical structure of the untreated and treated OPEFB, with dilute-acid hydrolysis in sulfuric acid at concentrations of 2, 4 and 6% for 30 min at 121°C, were examined with a scanning electron microscope (SEM) (Jeol JSM 5910LV XL,Jeol Ltd., Tokyo, Japan), operating at 15 kV and 29 Pa. The samples were dried at 60°C for 24 h and coated with 20 nm of gold and palladium (Hassan et al., 2013).

Experimental design

The response surface methodology (RSM) was used to optimize the hydrolysis process. The basic theoretical aspects, the fundamental assumptions and the experiment implications of RSM have been discussed elsewhere (Myers et al., 2009). A Box-

Behnken-based design was used with 30 runs and six replicates of the central point. The independent variables were sulfuric acid concentration [2, 4 and 6% (w/v)], contact time (20, 30 and 40 min), solid:liquid ratio (1:8; 1:10 and 1:12), and particle size (0.05, 3, and 4 cm). The xylose, glucose, acetic acid and HMF contents were taken as dependent variables in the production of fermentable sugars and inhibitors for the acid hydrolysis of OPEFB. For each of the dependent variables, a complete second order model of the equation was fitted (Equation 1).

$$Y = \beta_0 + \sum_{i=1}^{4} \beta_0 \left(X_i\right) + \sum_{i=1}^{4} \beta_{4+i} \left(X_i^2\right) + \sum_{i=i}^{4} \sum_{i'>i}^{4} \beta_{6+i+i'} \left(X_i X_{i'}\right), \qquad i = 1,2,3,4 \tag{1}$$

Where, Y represents the expected value of the response variable (xylose, glucose, acetic acid and HMF contents), β_i represent the estimated coefficients of the model, and X_1, X_2, X_3 and X_4 are the independent variables (acid concentration, contact time, solid:liquid ratio and particle size). The regression analysis was carried out using R software (Lenth, 2009). Fischer-test was used for determination of type of model equation, while the Student t-test was performed for determination of statistical significance of regression coefficients. For the xylitol concentration and Yp/s, a one-way analysis of variance (ANOVA) was used at a 5% significance level, considering the factor as type of strain: adapted and non-adapted. The least significant difference (LSD) was used to compare the treatments when significant differences were found. All analyses were performed using R software.

RESULTS AND DISCUSSION

Composition of empty fruit bunches

The cellulose and hemicellulose contents of the OPEFB were 45.36 and 28.83%, respectively, which makes this OPEFB a suitable raw material for the production of fermentable sugars. Other compounds, such as total lignin (21.87%), ash (1.90%), extractives in water (3.80%), extractives in ethanol (10.01%) and moisture (6.46%), were similar to those reported in the literature (Hamzah et al., 2011; Ferrer et al., 2013; Palamae et al., 2014). However, the differences seen in the OPEFB compositions as compared with other studies could be due to the maturity degree of the fresh fruit bunches, the geographic regions, and the soil conditions (Hazir et al., 2012).

OPEFB dilute-acid hydrolysis

Sugars, as xylose and glucose, were released during the dilute-acid hydrolysis, according to the experiment operating conditions, which are shown in Table 1. The maximum xylose concentration (32.59 g L^{-1}) was released when the reaction was carried out at 121°C for 30 min with an acid concentration maintained at 2%, solid:liquid ratio of 1:8 and 4 cm particle size. Under the same conditions, the inhibitor concentrations, such as HMF, glucose and acetic acid, were 0.023, 1.033 and 11.078 g L^{-1}, respectively. Hydrolysis procedures at high temperatures under acid conditions lead to the formation and release of acetic acid. The maximum acetic acid concentration (11.078 g L^{-1}) was seen with these conditions. On the other hand, the highest release of glucose (1.80 g L^{-1}) and the maximum concentration of HMF (0.038 g L^{-1}) were obtained at 121°C for 30 min, with the acid concentration maintained at 4%, a solid:liquid ratio of 1:8 and a 0.05 cm particle size.

OPEFB fibers have been used to produce xylose using dilute-acid hydrolysis, with the following optimum conditions: 1:10 solid:liquid ratio and sulfuric acid concentration between 0.25 to 0.5% (w/v). As the solid:liquid ratio increased, the xylose recovery was maximum at temperatures between 140 to 160°C (Zhang et al., 2012). Rahman et al. (2007) reported that the maximum xylose concentration (30.81 g L^{-1}) was seen when the reaction was carried out at 115°C for 60 min with an acid concentration of 4% and particle size <1 mm. This xylose concentration was similar to the data of this study, but with a different contact time (30 min) and particle size (3 cm). More importantly, similar xylose yields were obtained with a particle size of 3 cm, which is much higher than that used in the literature (less than 1 mm). Furthermore, Zhang et al. (2012) reported that, when the particle size was further reduced to 1 mm, the xylose yield dropped and the highest xylose production was obtained with a particle size of 2 mm. In this study, a high concentration of xylose was produced in the hydrolysate of the OPEFB, with large particle sizes and a low concentration of glucose. A large particle size and dilute-acid hydrolysis were probably not able to reduce the crystallinity of the cellulose, and the glucose concentration in the medium was less than that with smaller sizes of fiber (Goh et al., 2016).

Furthermore, the HMF, as an inhibitory compound exclusively produced with acetic acid by dehydrating hexoses, would hinder the microorganism growth in fermentation. Some studies have shown that lignocellulosic hydrolysates containing greater than 1 g L^{-1} of furfural or HMF had a significant inhibitory effect on the xylose fermentation using *Candida tropicalis* (Huang et al., 2011). Under this criterion, the formation of HMF during the dilute-acid hydrolysis of OPEFB could be ignored because it had relatively low concentrations, according to the maximum data of this study (0.038 g L^{-1}). Chiesa and Gnansounou (2014) reported an acetic acid concentration (1.53 g L^{-1}) when the hydrolysis was carried out at 161.5°C, 9.44 min and 1.51% acid sulfuric concentration. However, the severity of this compound was not particularly evident. This acid is probably of minor relevance with respect to the possible inhibition of microorganisms. In fact, concentrations up to 10 g L^{-1} have been found not to affect fermentation process (Mussatto and Roberto, 2004). Taking into account these results, detoxification procedures should be avoided

Table 1. Box-Behnken design (BBD) applied for the OPEFB dilute-acid hydrolysis and **t**he corresponding experiment responses used for the RSM modeling.

RUN	Coded variable*				Responses**			
	X1	X2	X3	X4	Y1	Y2	Y3	Y4
1	0	0	1	1	32.59	1.03	11.08	0.023
2	0	1	-1	0.5	19.83	0.55	6.18	0.011
3	-1	0	0	1	27.81	0.67	9.79	0.014
4	-1	0	1	0.5	30.16	0.97	9.68	0.020
5	1	0	0	1	23.78	0.97	9.80	0.026
6	1	1	0	0.5	24.88	1.04	10.36	0.023
7	0	0	0	0.5	26.43	1.03	8.68	0.031
8	0	0	0	0.5	27.38	1.03	8.27	0.031
9	1	-1	0	0.5	24.45	0.95	6.73	0.013
10	0	1	1	0.5	27.98	0.75	9.23	0.013
11	1	0	0	-1	23.32	1.67	8.23	0.035
12	-1	0	-1	0.5	22.65	0.53	7.68	0.024
13	-1	-1	0	0.5	24.17	0.53	6.89	0.004
14	1	0	1	0.5	29.09	1.47	10.48	0.033
15	1	0	-1	0.5	26.26	1.36	9.94	0.028
16	0	-1	0	-1	19.81	0.79	6.10	0.013
17	0	-1	-1	0.5	20.03	0.55	5.92	0.008
18	0	0	0	0.5	27.95	1.03	7.92	0.019
19	0	0	0	0.5	24.81	1.28	8.17	0.025
20	-1	1	0	0.5	25.75	0.51	8.47	0.003
21	0	0	1	-1	31.60	1.80	9.09	0.038
22	0	0	-1	1	22.76	0.69	7.86	0.021
23	0	0	-1	-1	22.67	0.91	7.01	0.015
24	0	-1	0	1	21.81	0.43	7.10	0.006
25	0	-1	1	0.5	29.40	0.79	8.60	0.015
26	-1	0	0	-1	22.03	1.19	7.16	0.022
27	0	0	0	0.5	25.27	0.90	8.10	0.015
28	0	1	0	1	23.25	0.53	6.81	0.010
29	0	0	0	0.5	25.86	0.93	8.78	0.023
30	0	1	0	-1	20.84	0.98	6.65	0.020

*X1, Acid concentration; X2, Contact time; X3, Solid:liquid ratio; X4, Particle size; **Y1, Xylose (g L^{-1}); Y2, Glucose (g L^{-1}); Y3, Acetic acid (g L^{-1}); Y4, Hydroxymethylfurfural (g L^{-1}).

under the conditions of this study. The estimation of the xylose yield over the independent variables X1, X2, X3 and X4 in terms of the response surfaces is shown in Figure 1. The optimum condition for the release of xylose from the OPEFB was set with the second-order polynomial model (Table 2), which was fitted to the experiment data and the regression coefficients were calculated with multiple regression analysis ($p<0.05$).

The model showed the relationship of the different parameters on the xylose recovery of the OPEFB where, the particle size of the samples (4 cm) was higher than that reported in similar studies with this material (Duangwang and Sangwichien, 2013; Hassan et al., 2013). The maximum xylose concentration of 32.59 g L^{-1} can be obtained by conducting a hydrolysis experiment with a 30 min reaction time, 2% acid concentration, solid:liquid ratio of 1:8, and 4 cm particle size, at a 121°C reaction temperature (Figure 1).

The regression analysis showed that the xylose, acetic acid, glucose and HMF production were significantly affected by the linear effect of solid:liquid ratio, negatively for the first two compounds, and positively for the latter two compounds, respectively, and by the quadratic negative effect of contact time (Table 2). Moreover, the glucose, acetic acid and HMF were linearly affected by variations in acid concentration and particle size. The glucose and HMF production were negatively affected by the interaction between solid:liquid ratio and particle size. In the case of correlation coefficients of the polynomial equation, the R^2 values were higher than 85%, which

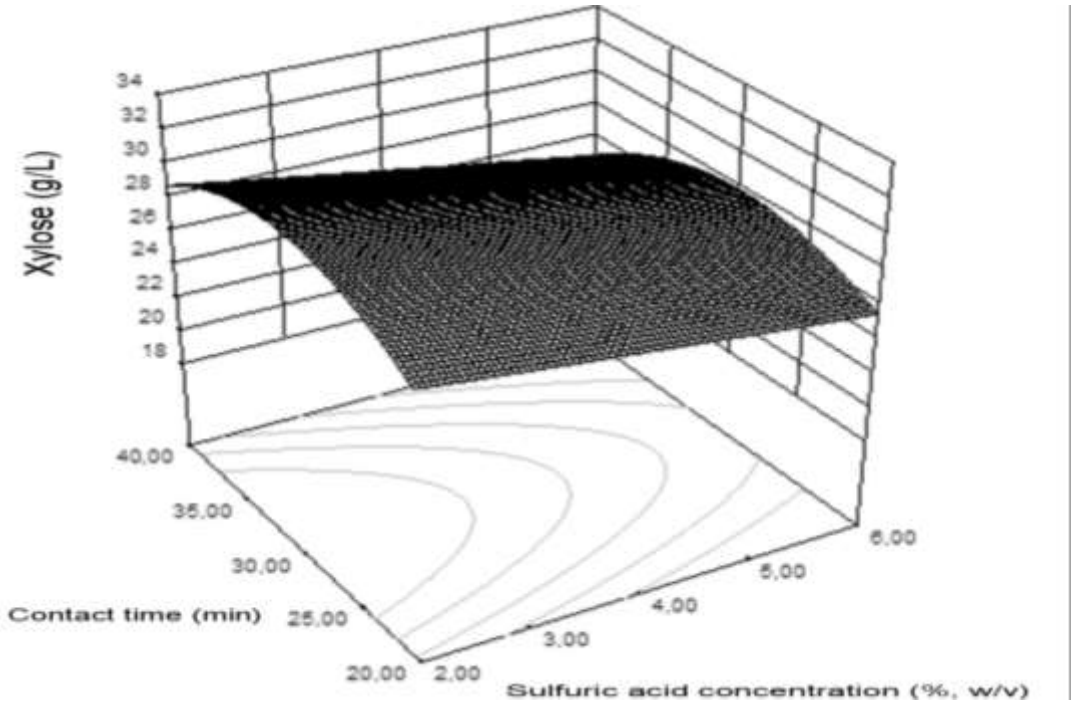

Figure 1. Production of xylose as a function of the acid concentration (%) and contact time when the solid:liquid ratio was maintained at 1:8 and the particle size was 4 cm.

Table 2. Regression equation coefficients and correlation coefficient (R^2) of the response surface models for xylose, glucose, acetic acid and HMF production from the OPEFB dilute-acid hydrolysis.

Variable and interaction*	Estimated regression coefficients			
	Xylose	Glucose	Acetic acid	HMF
β_0	-8.385	-5.224	4.886	-0.134
X_1	3.857	0.170†	-1.099†	-0.006†
X_2	1.886	0.227	0.640	0.008
X_3	-301.881†	26.198†	-165.953†	0.203†
X_4	3.235	0.491†	-0.039†	0.018†
X_1X_1	0.007	0.015	0.197†	0.000
X_1X_2	-0.014	0.001	0.002	0.000
X_1X_3	-28.052	-1.922	-8.789	0.050
X_1X_4	-0.222	-0.003	-0.033	-0.000
X_2X_2	-0.027†	-0.003†	-0.012†	-0.000†
X_2X_3	-1.45919	-0.045	0.452	0.006
X_2X_4	-0.003	-0.001	0.000	-0.000
X_3X_3	3138.79	14.156	1109.69	1.488
X_3X_4	-3.580	-4.156†	3.975	-0.144†
X_4X_4	-0.337	-0.028	0.020	-0.000
R-square (R^2) (%)	85.5	93.8	84.9	88.7

*X_1, Acid concentration; X_2, Contact time; X_3 , Solid:liquid ratio; X_4 , Particle size; β_0 is the intercept of quadratic model. †Significant at P<0.05.

indicated good agreement between experimental data and the model. Thus, the response could be sufficiently explained by the model. Figure 2 shows the 3D response surface plots constructed on the basis of Table 2. With regards to the OPEFB hydrolysis process, glucose, acetic acid and HMF were produced, but the low concentration

of these compounds would not affect the possible production of metabolites by fermentation with microorganisms. The 3D response surface plots represent a quadratic model, explaining the behavior of inhibitors, such as glucose, acetic acid and HMF, with determination coefficients (R^2) near to 0.93, 0.85 and 0.88, respectively.

The xylose production, taking into account variables such as particle size, solid:liquid ratio, sulphuric acid concentration and contact time during the hydrolysis process, is shown in Figure 1. The effects of the solid:liquid ratio and contact time were the more important factors for the released xylose. Furthermore, the maximum xylose concentration was reached with contact times close to 30 min and 2% sulphuric acid concentrations according to the model, where R^2 was 0.85, which explained 85% of the variability in the xylose response. These values are similar to other studies, where the acid hydrolysis of OPEFB fiber for the production of xylose was evaluated using RSM and a R^2 of about 0.83 (Rahman et al., 2007).

By applying the desirability function method, 29 solutions were obtained for the optimum criteria, with a desirability value in the range of 0.8 to 0.9 (Results not shown). The criteria for this optimization were the maximum xylose concentration, the minimum glucose concentration, and HMF and acetic acid in the test range. All of the conditions of the desirability functions were close to each other, for example, the sulphuric acid concentration varied between 2 to 2.2%, the contact time was in the range of 30 to 37.5 min, the solid:liquid ratio was 1:8 and the particle size was around 4 cm. Under these circumstances, the solution that had the highest xylose concentration values was selected. Therefore, the optimum process conditions with a desirability value of 0.9 were 1:8 solid:liquid ratio, 2% acid concentration and 4 cm particle size, at 121°C for 30 min. At this point, the xylose, glucose, HMF and acetic acid concentrations were calculated as 32.597, 0.769, 0.012 and 11.065 g L^{-1}, respectively.

Morphological changes of OPEFB

The micrographs of the OPEFB surfaces examined under SEM are shown in Figure 3. The G and H images showed the presence of silica bodies, which are formed by soil minerals moving into the sedimentary cavities between and within cell walls during plant growth. These structures have been found in great numbers in OPEFB (Hassan et al., 2013). Circular craters are completely filled with a solid, transparent silica body, which is silicon dioxide (SiO_2) (Ilvessalo-Pfaffli, 1995). A component, such as lignin, is a physical barrier for any lignocelluloses biomass. The presence of silica bodies on the OPEFB fiber surface is an additional resistance and increases the protective layer of the fiber, which obstructs the penetration of chemicals into the hemicellulose matrix and cellulose (Yunus et al., 2010). The dilute-acid hydrolysis could penetrate the lignin without other pretreatments and was able to remove the silica bodies. The presence of empty sedimentary cavities revealed perforations, which is shown in images E and F, when the fibers were treated with 4% sulfuric acid. However, the same effect was achieved with acid concentrations of 2 and 6%, where the silica bodies were removed, a breakdown of the OPEFB fibers was observed and a lot of the fiber surfaces were damaged. The acid hydrolysis with 2% sulfuric acid and a particle size of 4 cm were selected as the best optimization condition for xylose production from OPEFB (images A, B, C and D). This treatment had fibers with a homogenous surface and no silica bodies.

Xylitol production

The bioconversion of xylose to xylitol was carried out with adapted and non-adapted *C. guilliermondii* strains. The non-adapted strains could convert xylose to 10.3 ± 0.6 g L^{-1} xylitol with a yield of 0.43 g g^{-1}; whereas the adapted strains produced 6.8 ± 0.4 g L^{-1} xylitol with a yield of 0.31 g g^{-1}. The xylitol production and the yield were significantly ($p < 0.05$) higher for non-adapted strains, indicating that it is not necessary to make an adaptation of *C. guilliermondii* in the optimized hydrolysate of OPEFB. In addition, this study focused on maximizing the recovery of xylose contained in the hemicellulosic fraction of the OPEFB with the lower amount of inhibitors to increase the bioconversion to xylitol using *C. guilliermondii* without the need for detoxification.

Previous studies conducted with *C. guilliermondii* on hydrolysates of agroindustrial residues had different xylitol productions and yields. Arruda et al. (2011) performed a fermentation in Erlenmeyer flasks (125 ml) containing 50 ml of the medium (pH 5.5), on a rotary shaker at 200 rpm, 30°C for 120 h and used *C. guilliermondii* yeast in sugarcane bagasse hemicellulosic hydrolysate with 70 g L^{-1} xylose. They reported that the xylitol production and Yp/s were 40 g L^{-1} and 0.6 g g^{-1}, respectively. In addition, the xylitol production from sorghum forage hydrolysate using *C. guilliermondii* were carried out in 125 ml Erlenmeyer flasks containing 50 ml medium, under 200 rpm, at 30°C for 96 h, and the highest xylitol production and Yp/s were 15.45 g L^{-1} and 0.35 g g^{-1}, respectively (Camargo et al., 2015). The xylitol production was also performed with the same yeast in 250 ml Erlenmeyer flasks, containing 100 ml of brewer's spent grain hydrolysate; which were agitated in a rotatory shaker at 200 rpm, at 30°C for 96 h. The optimized conditions resulted in 0.78 g g^{-1} of Yp/s (Mussatto and Roberto, 2008). Therefore, the fermentation for xylitol production using different types of hydrolysate as carbon source can be affected by several factors such as, the

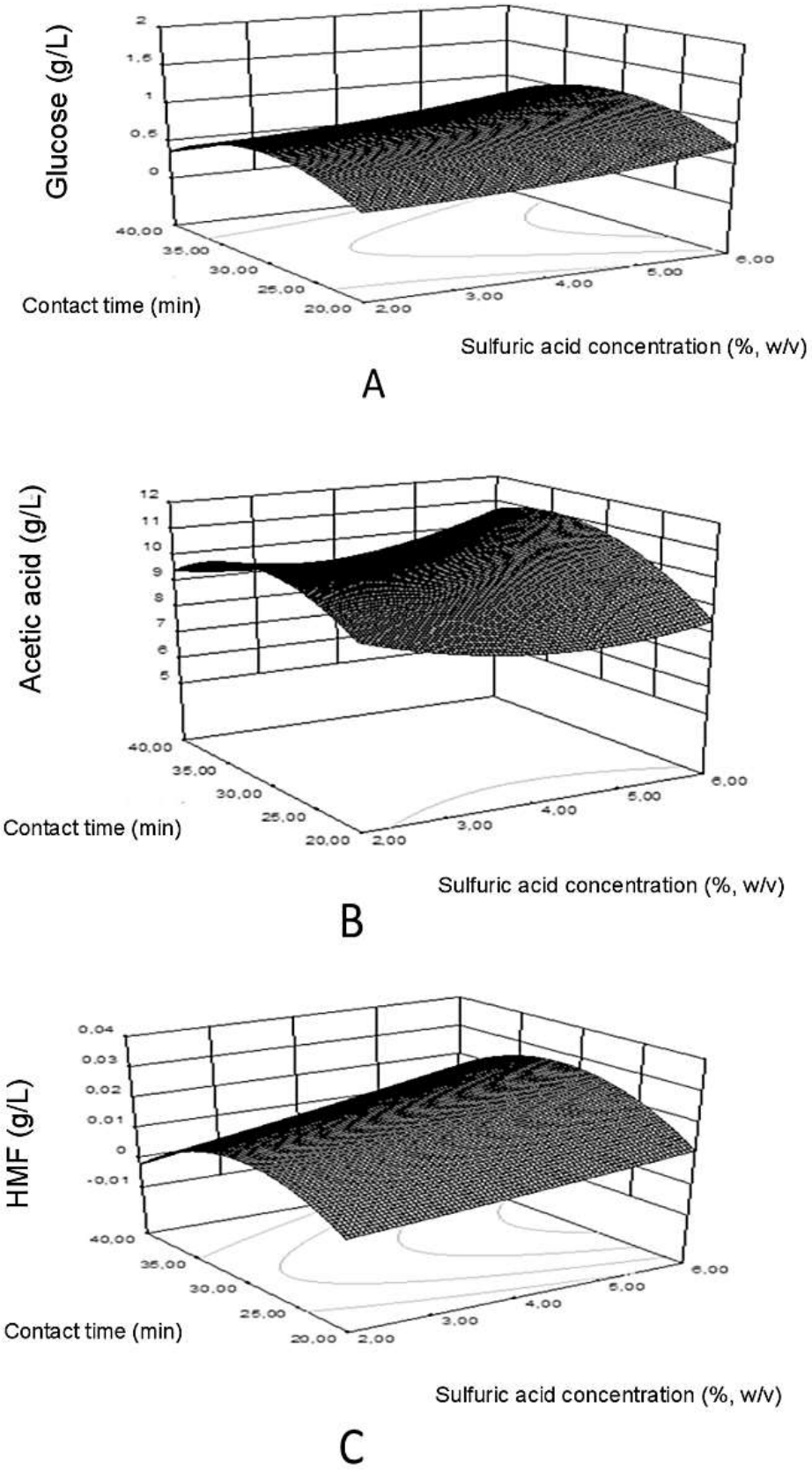

Figure 2. Production of glucose (A), acetic acid (B) and HMF (C) as a function of the acid concentration (%) and contact time (min) when the solid:liquid ratio was maintained at 1:8 and the particle size was 4 cm.

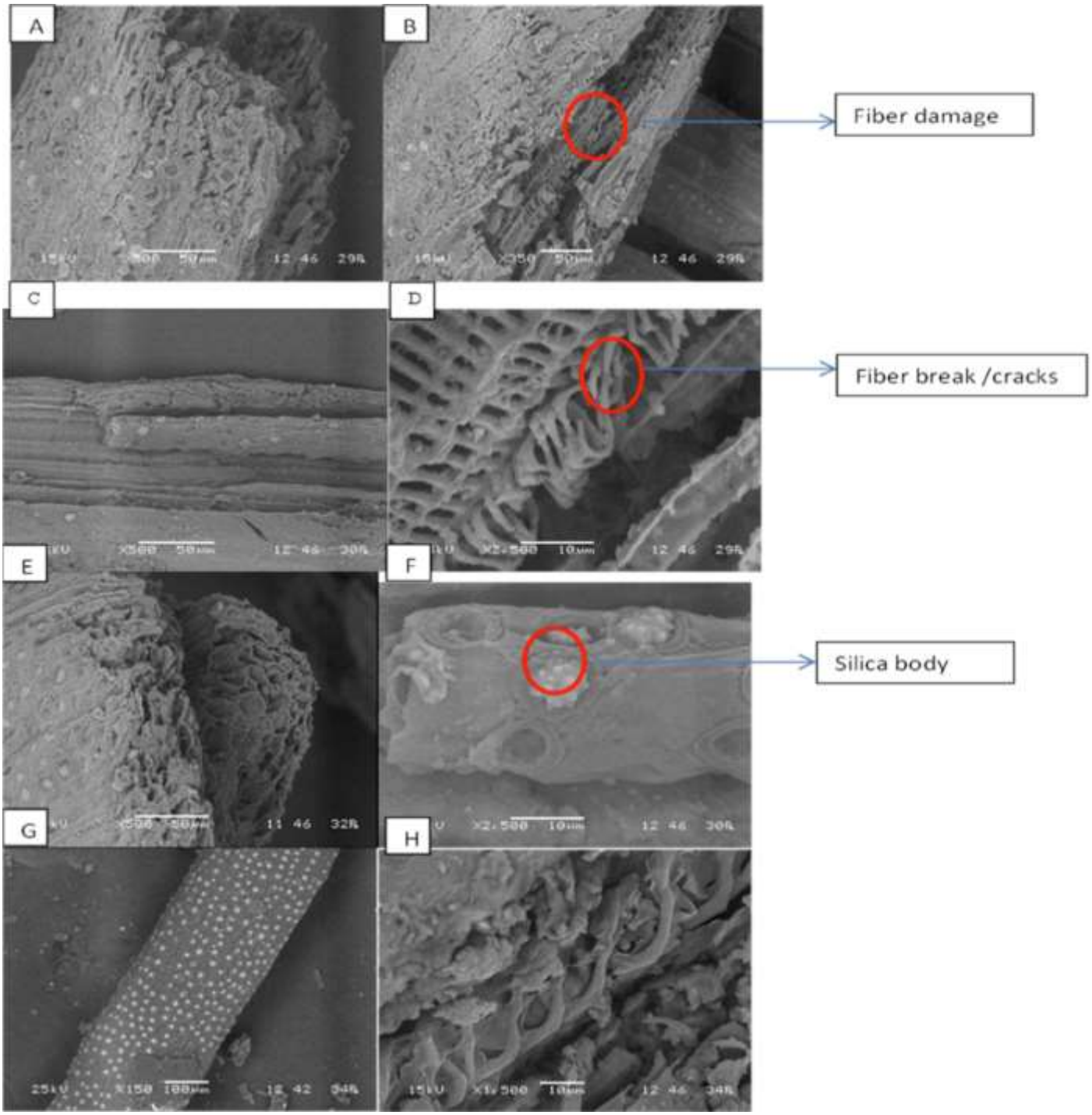

Figure 3. SEM images of the OPEFB pretreated with 2% sulfuric acid + 3 cm particle size (A and B), OPEFB pretreated with 6% sulfuric acid + 3 cm particle size (C and D), OPEFB pretreated with 4% sulfuric acid + 3 cm particle size (E and F) and the untreated OPEFB (G and H).

initial cell concentration, pH, temperature, type and concentration of nutrients in the culture medium, initial xylose concentration, presence of carbon sources other than xylose, the presence of inhibitor compounds in the hemicellulosic hydrolysates and the dissolved oxygen level (Silva et al., 1998; El-Baz et al., 2011; Salgado et al., 2012; Morales-Rodriguez et al., 2016).

The operational aspects of xylitol production and the cell metabolism are affected by the dissolved oxygen concentration, which is one of the most important

parameters to be considered in the production of xylitol (Salgado et al., 2012). An increase in xylitol productivity occurs when the oxygen supply is limited or the maximum oxygen supply is lower than the cell demand (Aguiar et al., 2002). Under anaerobic conditions, yeasts are unable to metabolize D-xylose. At a low oxygen level, the electron transport system is unable to oxidize intracellular nicotinamide adenine dinucleotide (NADH) completely, increasing the NADH concentrations and permitting xylitol excretion. At a high oxygen level, the oxidation favors xylitol oxidation to xylulose (Mohamad et al., 2015).

Walther et al. (2001) simulated different aeration conditions according to the levels of medium volume in 250 ml Erlenmeyer flasks. The medium volume at 26, 40 and 54% with respect to the Erlenmeyer flask volume was established for aerobic, semi-aerobic and microaerobic aeration, respectively. The medium volume used in the fermentation was 47%, which could be considered aeration with microaerobic tendency. Optimal values of oxygen concentration for xylitol production usually correspond to microaerobic conditions (Aguiar et al., 2002; Salgado et al., 2012). However, the strains grow vigorously at the beginning of fermentation at high initial xylose concentrations and high aeration. This leads to high cell densities and low oxygen levels in the later stages of the fermentation and results in high xylitol production rates. At lower initial xylose concentrations, cell densities are low and the level of dissolved oxygen remains high, therefore, less xylitol accumulates (Walther et al., 2001). Furthermore, extremely high initial xylose concentrations are detrimental to xylitol yields due to osmotic stress, which could be induced in the microorganism by the excess amount of sugar in the medium. Thus, with a careful manipulation of the both, the aeration and initial xylose concentration could result in high xylitol yields. In both the productivity and the yield of xylitol, aeration appeared to be a very important factor (Nolleau et al., 1993). If the fermentation medium contained glucose, then higher yields and productivities are obtained under aerobic conditions, while in the absence of glucose or with low initial glucose concentrations, microaerobic conditions improve yields. This behavior can be attributed to increased oxygen demand by the high cell densities achieved in the presence of glucose (Walther et al., 2001). The xylitol productivity from the optimized hydrolysate of OPEFB could be improved by controlling the dissolved oxygen in the flask. But, several factors should be taken into account, such as the initial concentration of xylose, glucose and strains.

Conclusion

The hydrolysis of the OPEFB fibers catalyzed by dilute sulfuric acid was optimized using a Box-Behnken-based design. The combination of operating at 121°C, for 30 min, with a 1:8 solid:liquid ratio, 2% acid concentration and 4 cm particle size was effective in terms of maximum xylose (32.597 g L^{-1}) and minimum glucose (0.769 g L^{-1}) concentrations, according to the prediction model. At these optimized conditions, the HMF and acid acetic concentrations were 0.012 and 11.065 g L^{-1}, respectively. However, when hydrolysis takes place at higher temperatures and higher acid concentrations, the presence of inhibitors can affect the rate of reaction during the fermentation process. Non-adapted *C. guilliermondii* strains were able to produce xylitol (10.3 ± 0.6 g L^{-1}) with a yield of 0.43 g g^{-1} from the optimized hydrolysate of OPEFB without detoxification. The xylitol productivity could be improved by controlling the dissolved oxygen in the flask and taking care of the initial concentration of xylose, glucose and strains.

CONFLICT OF INTERESTS

The authors have not declared any conflict of interests.

ACKNOWLEDGEMENT

Colciencias is acknowledged for providing a grant to Katherine Manjarres-Pinzón.

REFERENCES

Aguiar WB, Faria LFF, Couto MAPG, Araujo OQF, Pereira N (2002). Growth model and prediction of oxygen transfer rate for xylitol production from d-xylose by *C. guilliermondii*. Biochem. Eng. J. 12:49-59.

Aguilera A, Benitez T (1989). Microbiology synergistic effects of ethanol and temperature on yeast mitochondria. Curr. Microbiol. 18:179-188.

Alfaro A, Rivera A, Pérez A, Yáñez R, García JC, López F (2009). Integral valorization of two legumes by autohydrolysis and organosolv delignification. Bioresour. Technol. 100:440-445.

Arruda PV, Rodrigues RCLB, Silva DDV, Felipe MGA (2011). Evaluation of hexose and pentose in pre-cultivation of *Candida guilliermondii* on the key enzymes for xylitol production in sugarcane hemicellulosic hydrolysate. Biodegradation 22:815-822.

Camargo D, Sene L, Variz DILS, Felipe MGA (2015). Xylitol bioproduction in hemicellulosic hydrolysate obtained from sorghum forage biomass. Appl. Biochem. Biotechnol. 175:3628-3642.

Carvalho ML, Sousa JrR, Suarez CAG (2013). Kinetic study of the enzymatic hydrolysis of sugarcane bagasse. Braz. J. Chem. Eng. 30:437-447.

Chiesa S, Gnansounou E (2014). Use of empty fruit bunches from the oil palm for bioethanol production: A thorough comparison between dilute acid and dilute alkali pretreatment. Bioresour. Technol. 159:355-364.

Dhaliwal SS, Oberoi HS, Sandhu SK, Nanda D, Kumar D, Uppal SK (2011). Enhanced ethanol production from sugarcane juice by galactose adaptation of a newly isolated thermotolerant strain of *Pichia kudriavzevii*. Bioresour. Technol. 102:5968-5975.

Dominguez JM, Cao N, Gong CS, Tsao GT (1997). Dilute acid hemicellulose hydrolysates from corn cobs for xylitol production by yeast. Bioresour. Technol. 61:85-90.

Duangwang S, Sangwichien C (2013). Optimization studies on acid hydrolysis of pretreated oil palm empty fruit bunch for production of xylose by application of response surface methodology. Adv. Mater. Res. 699:77-82.

El-Baz AF, Shetaia YM, Elkhouli RR (2011). Xylitol production by *Candida tropicalis* under different statistically optimized growth conditions. Afr. J. Biotechnol. 10:15353-15363.
Fedepalma (2014). Producción de aceite de palma se incrementó 7% en 2013. Fed. Nac. Cultiv. Palma Aceite. 3.
Ferrer A, Requejo A, Rodríguez A, Jiménez L (2013). Influence of temperature, time, liquid/solid ratio and sulfuric acid concentration on the hydrolysis of palm empty fruit bunches. Bioresour. Technol. 129:506-511.
Goh KY, Ching YC, Chuah CH, Abdullah LC, Liou NS (2016). Individualization of microfibrillated celluloses from oil palm empty fruit bunch: comparative studies between acid hydrolysis and ammonium persulfate oxidation. Cellulose 23:379-390.
Hamzah F, Idris A, Shuan TK (2011). Preliminary study on enzymatic hydrolysis of treated oil palm (*Elaeis*) empty fruit bunches fibre (EFB) by using combination of cellulase and β 1-4 glucosidase. Biomass Bioenergy 35:1055-1059.
Hassan O, Ling TP, Maskat MY, Illias RM, Badri K, Jahim J, Mahadi NM (2013). Optimization of pretreatments for the hydrolysis of oil palm empty fruit bunch fiber (EFBF) using enzyme mixtures. Biomass Bioenergy 56:137-146.
Hazir MHM, Shariff ARM, Amiruddin MD (2012). Determination of oil palm fresh fruit bunch ripeness-based on flavonoids and anthocyanin content. Ind. Crops Prod. 36:466-475.
Hong E, Kim J, Rhie S, Ha SJ, Kim J, Ryu Y (2016). Optimization of dilute sulfuric acid pretreatment of corn stover for enhanced xylose recovery and xylitol production. Biotechnol. Bioprocess Eng. 21:612-619.
Huang CF, Jiang YF, Guo GL, Hwang WS (2011). Development of a yeast strain for xylitol production without hydrolysate detoxification as part of the integration of co-product generation within the lignocellulosic ethanol process. Bioresour. Technol. 102:3322-3329.
Ilvessalo-Pfaffli MS (1995). Fiber atlas: Identification of papermaking fibers, 1st edn. Springer Berlin Heidelberg, New York.
Kim S, Kim CH (2013). Bioethanol production using the sequential acid/alkali-pretreated empty palm fruit bunch fiber. Renew. Energy 54:150-155.
Lenihan P, Orozco A, O'Neill E, Ahmad MNM, Rooney DW, Walker GM (2010). Dilute acid hydrolysis of lignocellulosic biomass. Chem. Eng. J. 156:395-403.
Lenth RV (2009). Response-surface methods in R, using rsm. J. Stat. Softw. 32:1-17.
Liu S, Wang Q (2016). Response surface optimization of enzymatic hydrolysis process of wet oxidation pretreated wood pulp waste. Cellulose Chem. Technol. 50:803-809.
Manjarres-Pinzón K, Arias-Zabala M, Molina-Ramírez YA, Betancur-Nieto MI, Rodriguez-Sandoval E (2016). Producción de xilitol por *Candida guilliermondii* a partir de fermentación de residuos de palma de aceite. Rev. UDCA Actual. Divulg. Científica. 19:403-409.
Mardawati E, Wira DW, Kresnowati M, Purwadi R, Setiadi T (2015). Microbial production of xylitol from oil palm empty fruit bunches hydrolysate: The effect of glucose concentration. J. Jpn. Inst. Energy 94:769-774.
Martín C, Marcet M, Almazán O, Jönsson LJ (2007). Adaptation of a recombinant xylose-utilizing *Saccharomyces cerevisiae* strain to a sugarcane bagasse hydrolysate with high content of fermentation inhibitors. Bioresour. Technol. 98:1767-1773.
Miura M, Shimotori Y, Nakatani H, Harada A, Aoyama M (2015). Bioconversion of birch wood hemicellulose hydrolyzate to xylitol. Appl. Biochem. Biotechnol. 176:947-955.
Mohamad NL, Mustapa Kamal SM, Mokhtar MN (2015). Xylitol biological production: A review of recent studies. Food Rev. Int. 31:74-89.
Morales-Rodriguez R, Perez-Cisneros ES, de Los Reyes-Heredia JA, Rodriguez-Gomez D (2016). Evaluation of biorefinery configurations through a dynamic model-based platform: Integrated operation for bioethanol and xylitol co-production from lignocellulose. Renew. Energy 89:135-143.
Mussatto SI, Roberto IC (2004). Alternatives for detoxification of diluted-acid lignocellulosic hydrolyzates for use in fermentative processes: A review. Bioresour. Technol. 93:1-10.
Mussatto SI, Roberto IC (2008). Establishment of the optimum initial xylose concentration and nutritional supplementation of brewer's spent grain hydrolysate for xylitol production by *Candida guilliermondii*. Process Biochem. 43:540-546.
Myers RH, Montgomery DC, Anderson-Cook C (2009). Response surface methodology: process and product optimization using designed experiments, 3rd edn. John Wiley & Sons Inc., New Jersey. 704 p.
Nolleau V, Preziosi-Belloy L, Delgenes JP, Navarro JM (1993). Xylitol production from xylose by two yeast strains: Sugar tolerance. Curr. Microbiol. 27:191-197.
Oberoi HS, Vadlani PV, Brijwani K, Bhargav VK, Patil RT (2010). Enhanced ethanol production via fermentation of rice straw with hydrolysate-adapted *Candida tropicalis* ATCC 13803. Process Biochem. 45:1299-1306.
Palamae S, Palachum W, Chisti Y, Choorit W (2014). Retention of hemicellulose during delignification of oil palm empty fruit bunch (EFB) fiber with peracetic acid and alkaline peroxide. Biomass Bioenergy 66:240-248.
Piñeros-Castro Y, Velasco GA, Proaños J, Cortes W, Ballesteros I (2011). Producción de azúcares fermentables por hidrólisis enzimática de cascarilla de arroz pretratada mediante explosión con vapor. Rev. Ion 24:23-28.
Rahman SHA, Choudhury JP, Ahmad AL, Kamaruddin AH (2007). Optimization studies on acid hydrolysis of oil palm empty fruit bunch fiber for production of xylose. Bioresour. Technol. 98:554-559.
Roberto IC, Mussatto SI, Rodrigues RCLB (2003). Dilute-acid hydrolysis for optimization of xylose recovery from rice straw in a semi-pilot reactor. Ind. Crops Prod. 17:171-176.
Rocha MVP, Rodrigues THS, de Albuquerque TL, Gonçalves LRB, Macedo GR (2014). Evaluation of dilute acid pretreatment on cashew apple bagasse for ethanol and xylitol production. Chem. Eng. J. 243:234-243.
Saeed M, Khan H, Khan MA, Simjee SU, Muhammad N, Khan SA (2010). Phytotoxic, insecticidal and leishmanicidal activities of aerial parts of *Polygonatum verticillatum*. Afr. J. Biotechnol. 9:1241-1244.
Salgado JM, Converti A, Domínguez JM (2012). Fermentation strategies explored for xylitol production. In. Silva SS, Chandel AK (eds) D-Xylitol: Fermentative Production, Application and Commercialization, 1st edn. Springer Berlin Heidelberg, Berlin. pp. 161-191.
Sene L, Converti A, Zilli M, Felipe M, Silva S (2001). Metabolic study of the adaptation of the yeast *Candida guilliermondii* to sugarcane bagasse hydrolysate. Appl. Microbiol. Biotechnol. 57:738-743.
Shatalov AA, Pereira H (2012). Xylose production from giant reed (*Arundo donax* L.): Modeling and optimization of dilute acid hydrolysis. Carbohydr. Polym. 87:210-217.
Silva CJSM, Roberto IC (2001). Improvement of xylitol production by *Candida guilliermondii* FTI 20037 previously adapted to rice straw hemicellulosic hydrolysate. Lett. Appl. Microbiol. 32:248-252.
Silva SS, Felipe MGA, Silva JBA, Prata AMR (1998). Acid hydrolysis of *Eucalyptus grandis* chips for microbial production of xylitol. Process Biochem. 33:63-67.
Sluiter A, Hames B, Hyman D, Payne C, Ruiz R, Scarlata C, Sluiter J, Templeton D, Wolfe J (2008). Determination of total solids in biomass and total dissolved solids in liquid process samples biomass and total dissolved solids in liquid process samples. National Renewable Energy Laboratory. Golden, CO, NREL Technical Report No. NREL/TP-510-42621.
Sluiter A, Hames B, Ruiz R, Scarlata C, Sluiter J, Templeton D, Crocker D (2012). Determination of structural carbohydrates and lignin in biomass determination of structural carbohydrates and lignin in biomass. National Renewable Energy Laboratory. Golden, CO.
Tomás-Pejó E, Ballesteros M, Oliva JM, Olsson L (2010). Adaptation of the xylose fermenting yeast *Saccharomyces cerevisiae* F12 for improving ethanol production in different fed-batch SSF processes. J. Ind. Microbiol. Biotechnol. 37:1211-1220.
Walther T, Hensirisak P, Agblevor FA (2001). The influence of aeration and hemicellulosic sugars on xylitol production by *Candida tropicalis*. Bioresour. Technol. 76:213-220.
Yañez R, Garrote G, Díaz MJ (2009). Valorisation of a leguminous specie, *Sesbania grandiflora*, by means of hydrothermal fractionation. Bioresour. Technol. 100:6514-6523.

Yunus R, Salleh SF, Abdullah N, Biak DRA (2010). Effect of ultrasonic pre-treatment on low temperature acid hydrolysis of oil palm empty fruit bunch. Bioresour. Technol. 101:9792-9796.

Zhang D, Ong YL, Li Z, Wu JC (2012). Optimization of dilute acid-catalyzed hydrolysis of oil palm empty fruit bunch for high yield production of xylose. Chem. Eng. J. 181-182:636-642.

INTRODUCTION

Bacteria are present abundantly in soil and interact with the environment surrounding them for their survival. The availability of these bacteria is crucial for healthy plant growth where they provide beneficial conditions to the plant (Pandya and Desai, 2014). Some of the important conditions where they exert their beneficial roles are through production of phytohormones (such as auxin and gibberellic acid), siderophores and antimicrobial metabolites (Iqbal and Hasnain, 2013). *Pseudomonas*, *Bacillus*, *Enterobacter* and *Arthrobacter* species are among the genera of common plant growth promoting bacteria (PGPB) that are often studied and explored (Mohite, 2013; Pandya and Desai, 2014; Reetha et al., 2014). Among these, *Pseudomonas* spp. is more popular studied for its ability to produce auxin and gibberellic acid.

Both plant hormones are crucial for normal development, especially in root growth. Auxin also known as indole-3-acetic acid (IAA), is an important plant hormone in the regulation of plant development and production of longer roots and increased the number of root hairs which will directly increase nutrient uptake by the plant (Mohite, 2013). On the other hand, gibberellic acid (GA) is widely documented to be involved in seed germination, seedling emergence, flower and fruit growth and also promotion of root growth and root hair abundances (King and Evans, 2003; Sponsel, 2001).

From the diversity of Pseudomonads studied, *Pseudomonas putida* is well-known for its agriculture usage (Xie et al., 1996; Pattern and Glick, 2002; Rodriguez et al., 2014). For example in *Euphorbia pulcherrima* cultivars and *Brassica napus*, *P. putida* was found to have positively affected plant growth (Cheng et al., 2012; Rodriguez et al., 2014). In addition to the study on the usage, researchers had also studied the feasibility of encapsulating these bacteria to enhance its functionality and its survival rate (Rekha et al., 2007).

With the huge potential of using *P. putida* as in agriculture, this study proposes to further its functionality on *Brassica chinensis* var *parachinensis* (Choy sum) a common vegetable dish for most Chinese in Malaysia. In addition, the benefits to the microbial ecosystems will be explored.

MATERIALS AND METHODS

Samples collection and isolation of *Pseudomonas* spp.

Six soil samples were collected randomly from the MARDI Organic Farm. The soil was taken at 15 cm from the rhizosphere of the selected plants. The soil was kept in a zip lock bag and process upon reaching laboratory. Ten grams of the soil was mixed with 100 mL of sterile distilled water (sH_2O). The soil suspension was agitated vigorously at 250 rpm for 2 h. Hundred and fifty microliter of the soil suspension was pipetted and dispensed onto King's B Agar. The agar plates were incubated at 30 ± 2°C for 48 h. Emerging colonies from the agar plates were picked and sub-cultured onto fresh media plates.

Screening of IAA and GA_3 producing *Pseudomonas* spp.

For indole-3-acetic acid estimation, method used by Iqbal and Hasnain (2013) was followed with modification. Bacterial cell suspension was incubated at 30 ± 2°C for 48 h and the culture broth was adjusted to 10^6 CFU/mL prior to pipetting of 2 mL culture broth into Eppendorf tube and centrifuged at 10,000 rpm for 30 min. After centrifugation, 1 mL of the supernatant and 2 mL of Salkowski's reagent were mixed properly and placed in dark for 30 min. Development of pink color indicated IAA production and the amount of IAA was measured using Nanodrop spectrophotometer at wavelength of 530 nm. A standard curve with different concentrations was constructed using synthetic IAA (Sigma) used to determine the amount of IAA produced by each *Pseudomonas* spp.

Screening of GA_3 producing *Pseudomonas* spp. was done according to the method proposed by Panday and Desai (2014). Standard curve was constructed using synthetic GA_3 (Sigma) and measured using Nanodrop spectrophotometer at 254 nm.

Identification and characterization potential of *Pseudomonas* spp.

Isolation of DNA was conducted using Qiagen DNeasy DNA extraction protocol as suggested by the manufacturer. Polymerase chain reaction (PCR) parameter and conditions used for this study followed the optimization made by Jeffrey (2008) with the modification on the primers used. The 16S rRNA gene region was amplified using universal primers F8 (AGA GTT TGA TCM TGG CTC) and rP2 (ACG GCT ACC TTG TTA CGA CTT). PCR products obtained were subjected to purification using Vivantis GF-1 Gel DNA recovery kit following the protocol provided by the manufacturer. The purified PCR products were sent for sequencing at First Base Laboratories Sdn. Bhd., Selangor.

Results obtained from the sequencing were then compared with the databases from National Center for Biotechnology Information (NCBI). Biochemical characterization of *Pseudomonas* spp. was conducted using BIOLOG Gen III microplate according to the method described by the manufacturer (BIOLOG Inc.).

Preparation of alginate beads

The selected bacteria were grown in a 2 L conical flask containing 1 L of nutrient broth for 24 h with vigorous agitation at 250 rpm. Upon 24 h, the CFU/mL of bacteria were adjusted to 10^8 CFU/mL before the suspension was centrifuged at 10,000 rpm for 30 min. Cell pallet obtained was then washed with sH_2O to remove the excess nutrient broth before addition of the cell into 1 L of 3% (w/v) sodium alginate solution. The suspension was then stirred for 30 min to ensure proper mixing. The suspension was then dripped into 0.1 M calcium chloride ($CaCl_2$) solution. The beads formed were left in the $CaCl_2$ solution for 1 h before being washed with sH_2O to remove excess salt form during the process. The beads were then kept in 4°C until used.

Glasshouse trial

Two seeds were planted in each pot with 5 replicates and 2 cycles. Treatments were *Pseudomonas* spp. strain PF1P and control. Five pots were supplied with 2 g of *Pseudomonas* spp. strain PF1P beads every 15 days until harvested. *B. chinensis* var *parachinens* was harvested at 35 days after planting. The fresh and dry weight and root length of the plants for each treatment were recorded. The test was conducted in a randomized completely block design (RCBD).

Soil microbial activity and soil health evaluation

Each similar treatment was pooled together and mixed evenly; 100 g of the soil were taken and proceed with BIOLOG Eco Plate analysis according to the manufacturer's protocol (Biolog Inc.). Shannon's diversity index (*H*) and substrate richness (*S*) were calculated to determine the effect of the microbe application towards the microbial community in the soil. Shannon's diversity index was calculated based on the equation of $H = \Sigma(P_i \times \ln P_i)$, where by P_i is the proportional optical density of each wells at 96 h and *S* was calculated based on the number of different carbon substrate utilized by the microbial community (Wang et al., 2007). From the pooled soil, 500 g was scooped into ziploc bags and sent for analysis of its cation exchange capacity (CEC), conductivity, total organic matter and percentage of organic carbon.

Statistical analysis

Data were statistically analyzed with t-test at 95% confidence level.

RESULTS

Isolation of *Pseudomonas* spp.

A total of 50 *Pseudomonas* spp. were isolated from the 6 soil samples collected from 3 different rhizospheres of MARDI organic farm (Table 1). It was observed that banana rhizosphere contained the most population of bacteria compared to lettuce and chili (Table 1). Soil sample from lettuce recorded the lowest CFU/g and total number of bacteria isolated.

Table 1. Diversity of microbes isolated from different sources.

Source of soil sample	CFU/g soil	Number of microbes isolated
Banana	3×10^8	24
Chili	1.25×10^8	15
Lettuce	5×10^7	11

Screening for phytohormones activities, identification and characterization of *Pseudomonas* spp.

From the 50 isolates of bacteria tested, 30% of the bacteria produced IAA and 35% GA_3. It was observed that *Pseudomonas* spp. strain PF1P gave the highest IAA and GA_3 reading compared to the other *Pseudomonas* spp. isolated. *Pseudomonas* spp. Strain PF1P was later identified as *P. putida* based on their 16S rRNA gene sequence. *P. putida* strain PF1P was observed to utilize several carbon sources such as gentiobiose, D-turanose, D-melibiose, α-D-glucose, D-mannone, D-fructose, L-fucose, L-lactic acid, Tween 40, D-galactose, D-fructose, L-fucose, D-gluconic acid, and α-keto-glutaric acid and citric acid (Table 2).

Table 2. Biochemical characterization of *Pseudomonas putida* strain PF1P.

Substrate	PF1P	Substrate	PF1P
Gentiobiose	+	Sucrose	-
D-Turanose	+	Stachyose	-
D-Melibiose	+	β-Methyl-D-glucoside	-
N-Acetyl-Neuraminic acid	-	D-Galactose	+
α-D-glucose	+	D-Fucose	+
D-Mannose	+	L-Rhamnose	-
D-Fructose	+	L-Fucose	+
D-Sorbitol	-	D-Mannitol	-
D-Arabitol	-	myo-Inositol	-
Glycerol	-	D-Gluconic acid	+
L-Lactic acid	+	α-Keto-Glutaric acid	+
Tween 40	+	α-Keto-Butyric acid	-
L-Alanine	-	L-Arginine	-
D-Serine	-	D-Aspartic acid	-
L-Serine	-	Citric acid	+

+: Utilized by *Pseudomonas putida* strain PF1P; -: not utilized by *Pseudomonas putida* strain PF1P.

Efficacy of *P. putida* strain PF1P on glasshouse trial

From the trial conducted, it was observed that *P. putida* strain PF1P increased the fresh weight of the *B. chinensis* var *parachinensis* by 54.6% and encouraged the elongation of roots by 51.3%. T-test conducted showed significant results on the increased of *B. chinensis* var *parachinensis* weight and root elongation at the confidence level of 95%. The average fresh weight, dry weight and root length are shown in Table 3.

Table 3. Effect of *Pseudomonas putida* strain PF1P on root length, fresh plant weight and dried plant weight.

Treatment	Root length (cm)	Fresh plant weight (g)	Dried plant weight (g)
Control	16.14 ± 0.46	38.12 ± 0.80	3.92 ± 0.19
Pseudomonas putida strain PF1P	18.76 ± 0.51	58.92 ± 0.80	5.93 ± 0.16

Mean ± standard deviation .

Effect of *P. putida* strain PF1P on soil microbial activity and soil health

It was observed that *P. putida* strain PF1P did not have any detrimental effect on the soil health when the results are compared to the control. Shannon's diversity index (*H*) calculated for soil inoculated with *P. putida* strain PF1P was observed to be 2.903 as compared to the control of only 2.635 (Table 4). Soil treated with *P. putida* strain PF1P showed higher CFU (5×10^9 CFU/g) compared to control of only 9×10^7 CFU/g (Table 4). There are no significant differences in the substrate richness (*S*) for both soil inoculated with *P. putida* strain PF1P and control. It was observed that organic matter and organic carbon content for treated soil sample increased by 5 and 3% respectively as compared to non-treated soil. The pH reading for treated soil did not show any significant changes similar to results obtained for CEC, conductivity and pH, respectively (Table 5).

Table 4. Effect of *Pseudomonas putida* strain PF1P on Shannon's diversity index (*H*), substrate richness (*S*) and colony forming unit per gram of soil (CFU/g).

Treatment	Shannon's diversity index (*H*)	Substrate richness (*S*)	Colony forming unit per gram of soil (CFU/g)
Control	2.635 ± 0.021[a]	32	9×10^7
Pseudomonas putida strain PF1P	2.903 ± 0.022[a]	32	5×10^9

[a]Standard deviation of the mean.

Table 5. Soil chemical properties before and after treatment of *Pseudomonas putida* strain PF1P.

Parameter	Before planting		After planting	
	Control	Treated with *P. putida* strain PF1P	Control	Treated with *P. putida* strain PF1P
Cation Exchange Capacity (meq/100 g soil)	5.06	5.12	4.90	4.86
pH	7.2	6.98	7.34	7.35
Conductivity (us/cm)	271.10	286.90	168.65	168.40
Organic carbon (%)	1.80	1.85	1.75	1.91
Organic matter (%)	3.30	3.38	3.15	3.55

DISCUSSION

IAA and GA_3 producer by *Pseudomonas*

In this study, *P. putida* strain PF1P showed a slightly higher IAA secretion of approximately 42.1 µg/mL as compared to studies done by Pattern and Glick (2002) where they only recorded IAA secretion of 32.7 µg/mL. In another study conducted by Reetha et al. (2014), *Pseudomonas fluorescens* isolated from the rhizosphere of onion produced only 15.38 µg/mL of IAA. According to Pattern and Glick (2002), the high reading of IAA content was correlated to the accumulation of indolepyruvic acid which reacted with the Salkowski's reagent. Puga-Freista et al. (2012) however observed that production of auxin was closely related to the host plants and growth of other soil organisms such as earthworms.

P. putida strain PF1P which was isolated from banana rhizosphere gave a GA_3 reading of 10.1 µg/mL. This result was slightly higher than the results obtained by Verma et al. (2016) from *P. putida* (9.8 µg/mL) and *P. flourescens* (6.64 µg/mL) isolated from Cuddalore district in India. Ambawade and Pathade (2015) noted that production of high gibberellic acid from *Bacillus siamensis* BE 76 was related to the host plant. In the study, *B. siamensis* BE 76 isolated from banana rhizosphere gave better GA_3 production. This might be due to secretion of certain stimulus by the banana plants that was not present in other plant.

Efficacy of *P. putida* strain PF1P on glasshouse trial

The increase of *B. chinensis* var *parachinensis* fresh weight as shown in Table 3 might be due to the increase in the absorption of nutrients and water by the root system of the plant. This could be caused by the colonization of the bacteria on the roots and the rhizosphere that encourage the absorption of minerals by plants through the development of more elongated and nested root structure (Rodriguez et al., 2014). This result correlates with *P. putida* strain PF1P, which caused a 51.3% increase in root elongation. Furthermore, treated *B. chinensis* var *parachinensis* showed the formation of plenty of root hairs at the primary and secondary roots. Study done by Pattern and Glick (2002) also supported the role of *P. putida* in increasing the rooting system of *Vigna radiate.*

Effect of *P. putida* strain PF1P on the soil microbial activity

Shannon's diversity index showed that soil treated with *P. putida* strain PF1P gave higher microbial activities and diversity as compared to the control. These phenomena could be classified as "rhizosphere effect" whereby colonization of *P. putida* strain PF1P could have secreted certain compounds in the plant rhizosphere and enhanced different microbial populations in the ecosystem (Rekha et al., 2007). This was observed in the increase of CFU/g count in soil inoculated with *P. putida* strain PF1P (Table 4).

Conclusion

P. putida strain PF1P isolated from the rhizosphere of banana plot was observed to be producing both IAA and GA_3. Encapsulated *P. putida* strain PF1P was able to enhance the rooting system and soil microbial diversity in glass house test. *P. putida* strain PF1P was also found to be non-detrimental to its microbial ecosystem and could be formulated with other fertilizers to reduce the dependency on chemical fertilizers.

CONFLICT OF INTERESTS

The authors have not declared any conflict of interests.

academicJournals

Vol. 16(41), pp. 2014-2023, 11 October, 2017
DOI: 10.5897/AJB2016.15813
Article Number: A9DB3EA66266
ISSN 1684-5315

http://www.academicjournals.org/AJB

African Journal of Biotechnology

Full Length Research Paper

Potentiality of lytic bacteriophages and their virolysins in lysing multi-drug resistant *Salmonella typhi*

Ayman A. Elshayeb*, Abdelazim A. Ahmed, Marmar A. El Siddig and Adil A. El Hussien

Department of Microbiology, Faculty of Sciences and Technology, University of Khartoum, Khartoum, Sudan.

Received 27 November, 2016; Accepted 24 February, 2017

Bacteriophage virolysins or lytic enzymes are bacterial peptidoglycan hydrolases responsible for lysing bacterial cells. Consequently, they are used as enzybiotics alongside with bacteriophage therapy to remedy multi-drug resistant *Salmonella typhi*. The objective of this study was to evaluate the potentiality of lytic bacteriophages and their virolysins in curing multi-drug resistant *S. typhi*. *S. typhi* was isolated and identified according to WHO and ISO guidelines. Antibiotics susceptibilities were tested using CLSI recommendations. Correspondingly, bacteriophage-lysing efficiency was assayed by plaques formation using the double-layer agar technique. Virolysins were extracted using ultracentrifugation and purified by dialysis after buffering in ammonium sulfate. Virolysins activity was determined by measuring the reaction mixtures spectrophotometrically (bacteria incubated as substrate in 37°C for 4 h). The phages and virolysins kinetics exponential rates were calculated using specific differential equations. Susceptibility data plotted based on antibiogram criteria confirmed that 33% of *S. typhi* isolates were multi-drug resistant. For bacteriophage replication and multiplicity of infection, phages were amplified to produce the maximum particles of titers. The phage titration data fit on sonogram revealed exponential decay of *S. typhi* incubated for 12 h. Meanwhile, the enzyme kinetics exponential decay on double reciprocal plot showed irretrievable relationship of host decay in 4 h. Since phages depend on their lytic cycle in lysing bacterial host, their enzymes have more capability in decaying the host; besides they are safe and time-saving when used in the treatment of antibiotics resistant *S. typhi*.

Key words: Antibiotics, bacteriophage, enzybiotics, *Salmonella typhi,* virolysins.

INTRODUCTION

With the emergence of multi-drug resistant (MDR) strains of *Salmonella typhi* worldwide, the increasing incidence of enteric fever leads to death, especially in poor communities (Gupta et al., 2009; Weill, 2010; Feasey et al., 2015). *S. typhi* rapidly gained resistance to antibiotics like ampicillin, chloramphenicol and cotrimoxazole; also the earlier efficacious drugs of fluoroquinolones like ciprofloxacin acquired a reduced sensitivity against MDR

*Corresponding author. E-mail: ayman_elshayeb@yahoo.com. Tel: +249122974208.

S. typhi as many cases reported (Madhulika et al., 2004; Jones et al., 2014). Therefore, bacteriophage therapy is an alternative drug to cure bacterial infections because they are highly specific in lysing bacteria, they do not contain integrated genes in their genomes and cannot coexist with the host and carry virulent genes from one host after decay to infect another (Borris et al., 2001). Phage therapy is the application of bacteriophages to bacterial infections of humans (or other animals) with the goal of reducing bacterial load. Phage therapy is complicated by the self-replicating nature of phage (Patel et al., 2011).

Bacteriophage virolysins including lysins, endolysins and lysozymes seem to be the most promising alternative antibiotics as a result of a few unique characteristics of this group of lytic enzymes (so-called enzybiotics). This word is coined to describe a treatment, which uses purified phage-encoded enzymes as antibacterial agents (Yang et al., 2014; Meaney et al., 2015). Virolysins are bacteriolytic agents that cause bacterial lysis by cleaving to bonds in the cell wall. They are presumed to be a phage-induced enzyme participating in lysis through its destructive action on the host cell wall (Courchesne et al., 2009). The peptidoglycan network is responsible for cell rigidity and containment of the cytoplasmic membrane. They share the specificity found in the bacteriophage in which it was produced during its lytic cycle (Skariyachan et al., 2016). Using phage-encoded bacterial cell wall virolysins to eliminate pathogenic bacteria has led to the designation of muralytic enzymes as enzybiotics. There are tremendous reviews that have dealt with the characteristics of virolysins and their applications as alternative enzybiotics in medical-oriented *in vitro* and *in vivo* tests (Maszewska, 2015). Although, lytic enzymes are more efficient for the lysis of Gram-positive bacteria, they also assist the lysis of Gram-negative bacteria such as *Salmonella* and *Shigella* (Ahluwalia et al., 2012; Bryan et al., 2016). Phage virolysins involved in the lytic cycle of phage replication have two classes of peptidoglycan hydrolase enzymes, namely, endolysins and virion associated hydrolase. They are characterized as phage-encoded proteins (Salazar and Asenjo, 2007). Bacteriophages encode holins and lysins to achieve their exit from the host bacteria. They form pores in the cytoplasmic membrane, following lysins accumulated in the cytoplasm and degrade the peptidoglycan layer. Damage to this layer results in cell rupture and concomitant virus released through loss of osmotic integrity (Buyuktimkin and Saier, 2015; Buyuktimkin and Saier, 2016).

Virolysin catalyzes the hydrolysis of 1, 4-beta-linkages between N-acetylmuramic acid and N-acetyl-D-glucosamine residues in peptidoglycans and between the N-acetyl-D-glucosamine residues in chitodextrins (Narasimhan et al., 1988). However, virolysins are promising enzybiotics for bacterial cell wall hydrolases even if these bacteria are resistant to lysozymes. They have narrow spectra of sensitive bacteria, minimizing the disturbance to normal microflora and a tremendous diversity of lytic bacteriophages in the biosphere, which guarantees their ability of targeting almost any bacteria (Filatova et al., 2015). To determine the kinetics exponential decay of virolysins mathematically, the resulting data points of equations were fit to curves solved on double reciprocal plot (Courchesne et al., 2009). Meanwhile, the bacteriophage values of kinetic lysing rate are usually obtained from the exponential growth data sets plotted on sensorgrams (Groman and Suzuki, 1963; Ploss and Kuhn, 2010). Clinical trials conducted to assess the safety and pharmacokinetic properties of virolysins confirmed that they are safe for humans and can enhance the lysing *S. typhi;* so they are highly recommended to be used for antibiotics resistant bacterial infections (Lopez-Cuevas et al., 2011). In the recent study, the potentiality of bacteriophages' virolysins lysing efficiency was evaluated and used *in vitro* as antimicrobial agents against multi-drug resistant *S. typhi.*

MATERIALS AND METHODS

Microorganisms' isolation and identification

S. typhi was recovered from Khartoum Wastewater Station. Cultural characteristics, biochemical and serological tests were performed according to the recommendations of ISO 6579 standard optimized by Mainar-Jaime et al. (2013). Each bacterium was tested for its susceptibility using National Committee for Clinical and Laboratory Standards Institute guidelines (CLSI, 2012). *S. typhi* allied lytic phages were isolated using the double-layer agar technique recommended by Mooijman et al. (2001).

Bacteriophages multiplicity of infection [MOI]

For lysing, *S. typhi* isolates lytic phages (with MOI = 50 phage/cell) were added to 5 ml of *S. typhi* culture in exponential growth phase until turbidity decreased (OD_{600nm}>0.3). The MDR-*S. typhi* allied phages' concentrations in the sample were amplified and maximized using plaque assay on double-layer agar technique. In it, bacteria were inoculated for the second time using serial dilutions of 10^{-8}, 10^{-9} and 10^{-10}; to release progeny phages, multidrug resistant *S. typhi* (I = 16 and R ≥32 µg/ml) was used as a host bacterial strain and stored at 4°C. When the OD_{600nm} was below 0.3, the inocula were filtered through 0.45 µm Whatman filter paper. The filtrates were collected in screw cap bottles containing 50 ml SM buffer which was prepared by dissolving 2.0% w/v gelatin, 2.0% w/v $MgSO_4.7H_2O$, 5.8% w/v NaCl in 200 ml tris HCl (1M, pH 7.5); the demineralized water volume was completed to 1.0 L.

Extraction of virolysins (lytic enzymes)

The bacteria-free filtrates were kept at 30°C without stirring for 2 days to sustain the phages' infection and replication before extracting the enzymes from the virion particles. Virolysins were extracted by centrifugation at 6,010 g for 30 min; ammonium sulfate (up to 40%) was added as a buffer to the supernatant and gently

mixed for 4 h at 4°C. The filtrates were sealed in dialysis bags (molecular weight cutoff, 12,000 to 14,000), and dialyzed at 4°C for 2 days against deionized water to purify the enzyme (Savary et al., 2001).

Detection of enzyme activity

Bacterial cultures were prepared and used to detect the lytic bacteriophages' virolysins activity. The enzymes were added to the culture (5 µg/ml) with a final proportion of 1:20 and incubated at 37°C for 4 h at OD_{600nm}. The enzyme activity was determined by measuring the reducing sugars released from lysed bacterial cells used as substrate in the reaction solution using Benedict's reagent.

Enzyme kinetics exponential decay

Salmonella typhi was added as a substrate (initial amount 1.0×10^6 cell/ml) to the extracted enzyme and incubated at 37°C for 4 h. The change in the mixture turbidity was recorded. The lysis rate was expressed as a reduction in the turbidity; it resembled the enzyme kinetics exponential decay rate $V = (\frac{dy}{dt} = -\lambda x)$.

RESULTS

Patterns of multi-drug resistant *S. typhi*

From the recovered bacteria species, 128 were identified as *S. typhi.* The isolates were tested for their susceptibility against antibiotics. The means of n=42 (33.0%) of the isolates were found to be multi-drug resistance and categorized in 8 main groups, namely, *S. typhi* 16, *S. typhi* 32, S.7 16, S.7 32, Dr11 16, Dr11 32, Sal C 16, and Sal C 32, based on the collection. The Minimum Inhibitory Concentrations (MICs) were determined at 16 and 32 µg/ml concentrations and 67.0% isolates that resist ciprofloxacin as Minimum Bactericidal Concentration (MBCs).

Antibiogram or *in vitro*-sensitivity showed patterns of *S. typhi* isolates that have developed resistance against most antibiotics (MDR), including ciprofloxacin and was interpreted as MBC ≥ 32 µg/ml (Figure 1).

Bacteriophage multiplicity of infection and amplification

The specific bacteriophage for each of the *S. typhi* was determined using the plaque assay. Phages were harvested at various intervals time and assayed by double-layer plaque assay on *S. typhi* lawn. This contributes significantly to the phage amplification by providing substrates for phage growth (Table 1). The multiplicity of infection of 50 phage/cell was assessed for the lysing of initial amount ($n\times10^6$ cell/ml) of the host, and the progeny phages released during the phage lytic cycle in 12 h incubation were amplified from $n\times10^{+8}$ up to $n\times10^{+11}$ phage/ml, where n = numerical digit.

Since the highest number of the plaques was obtained at high titers that correlated to the initial number of bacterial cells, then initial amounts of *S. typhi* isolates ($n\times10^6$) were infected by their lytic phages (MOI = 50 phage/cell) and replicated for titer (10^8). To obtain the maximum numbers of phage's cells per sample amplified for 12 h at 37°C, the numbers of phages' plaques (pfu/ml) were recorded for titers 10^{-8} up to 10^{-9} and 10^{-10}.

Bacteriophage exponential lysing rate

The capacity of phage to lyse bacterial lawns producing high numbers of pure plaques occurred when higher titers were selected after 12 h of incubation. To calculate the phages potentiallity in lysing *S. typhi* per serial dilution, the bacteria were tittered at 10^{-8}, 10^{-9} and 10^{-10} using the formula: [$y = a .10^n e^{(bx)}$], where a = exponential constant, 10^n = titer, e = exponential number and (x) = plaque formation/isolate at certain point (Figure 2).

The exponential portion of the curve was used to determine the slope of lysing rate and the data were used to calculate the decrease in OD_{600} per unit of time. The bacteriophage amplification rate given by [$y = (2\times10^{+9}) e^{0.2908x}$, $y = (2\times10^{+10}) e^{0.02085x}$ and $y = (7\times10^{+11}) e^{0.0373x}$] and their Spearman's rank correlation coefficient (R^2) = 0.5, 0.4 and 0.1 are in low values.

Bacteriophage kinetics titrations

The phage lysing rates of their host were determined by the time needed for bacteria to produce phages after infection and decreasing of optical density (OD_{600nm}) per minute. To confirm the phage specificity toward the specific bacteria, the numbers of plaques/phages increased for each isolate by increasing their titration rates (Equations 1 to 5).

The kinetic titration given by:

$$A+B \overset{ki}{\rightleftharpoons}_{kd} AB \quad (1)$$

$$\frac{dA}{dt} + \frac{dB}{dt} \overset{ki}{\rightleftharpoons}_{kd} \frac{d(AB)}{dt} \quad (2)$$

[A] = Initial amount of Salmonella (10^6 cell/ml), [B] = Phages ([MOI = 50 phage/cell], [LA]=concentration of reaction mixture, k_i= Initial kinetics absorbance (OD_{600nm} = 1), k_d= decreasing kinetics absorbance rate (OD_{600}<0.3). The k called rate constants are constants of proportionality in the application of the Law of Mass Action. Response was calculated for bacteriophage exponential kinetics titration: where R = replicated titer, t= total time of incubation and t_0 = initial time of incubation.

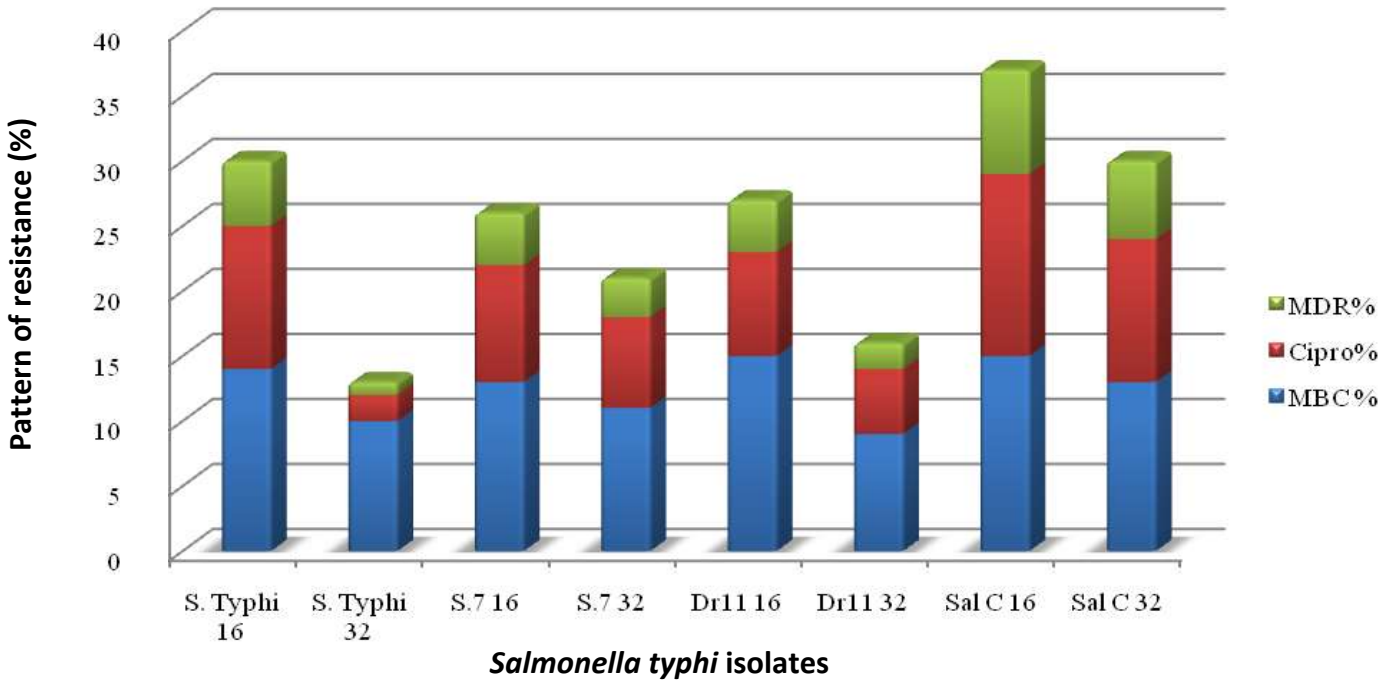

Figure 1. Antibiogram criteria for multi-drug resistant strains. *MDR: Multi-drugs, Cipro: ciprofloxacin, MBC: minimum bactericidal concentration.

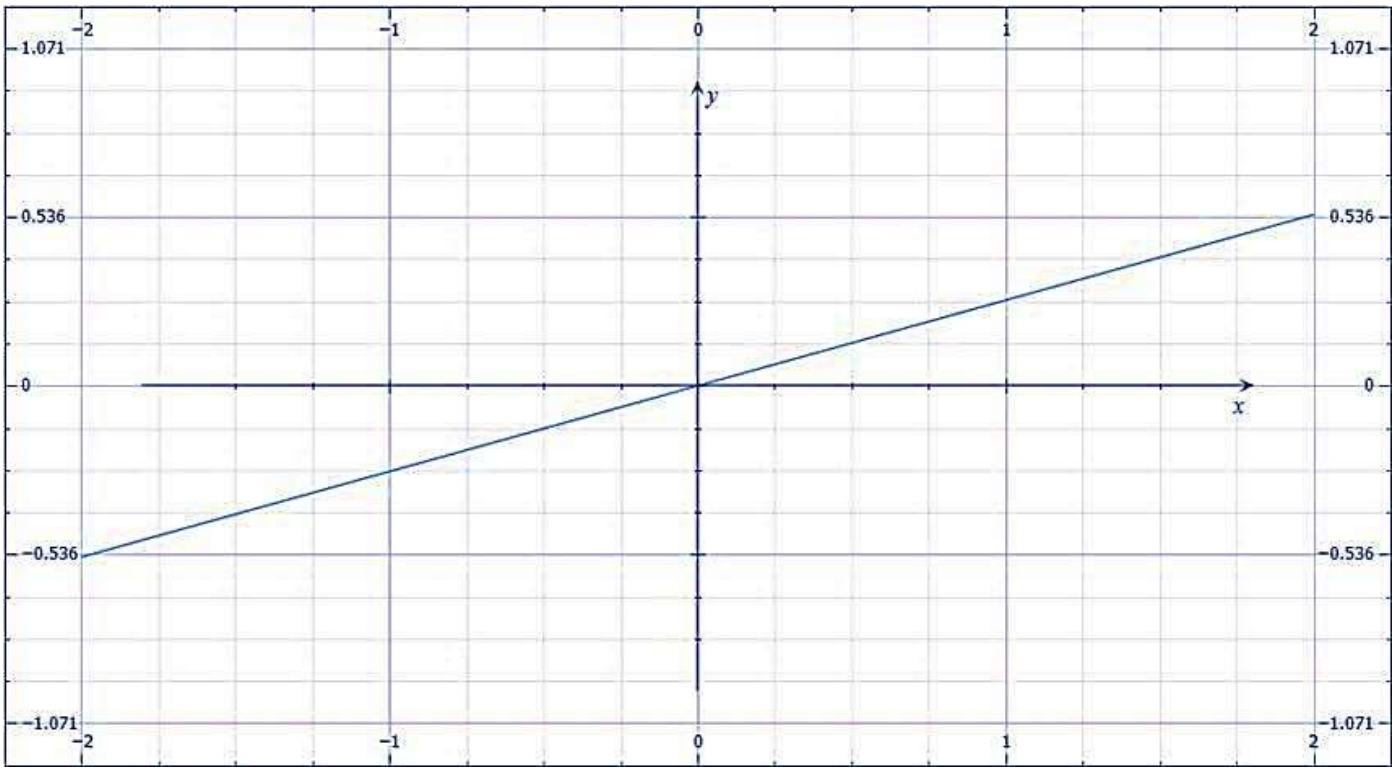

Figure 2. Plotting the slope of bacteriophages' amplification rates.

Table 1. Bacteriophage lytic replication and amplification to get the highest numbers of phage cells/sample.

Salmonella **(Initial amount OD $_{600nm}$ = 1)**	**cell/ml**	**Bacteriophage**								
		Dilution	**Plaques**	**PFU/ml**	**Dilution**	**Plaques**	**PFU/ml**	**Dilution**	**Plaques**	**PFU/ml**
S. typhi 16	1.6×10^{6}	10^{-8}	62.0	6.2×10^{9}	10^{-9}	42.0	4.2×10^{10}	10^{-10}	52.0	5.2×10^{11}
S. typhi 32	2.8×10^{6}	10^{-8}	78.0	7.8×10^{9}	10^{-9}	80.0	9.0×10^{9}	10^{-10}	84.0	8.4×10^{11}
S.7 16	1.7×10^{6}	10^{-8}	46.0	4.6×10^{9}	10^{-9}	66.0	6.6×10^{10}	10^{-10}	94.0	9.4×10^{11}
S.7 32	1.1×10^{6}	10^{-8}	58.0	5.8×10^{9}	10^{-9}	64.0	6.4×10^{10}	10^{-10}	78.0	7.8×10^{11}
Dr11 16	9.0×10^{5}	10^{-8}	90.0	9.0×10^{9}	10^{-9}	88.0	8.8×10^{10}	10^{-10}	96.0	9.6×10^{11}
Dr11 32	1.3×10^{6}	10^{-8}	74.0	7.4×10^{10}	10^{-9}	76.0	7.6×10^{10}	10^{-10}	58.0	5.8×10^{11}
Sal C 16	1.5×10^{6}	10^{-8}	24.0	2.4×10^{10}	10^{-9}	86.0	8.6×10^{10}	10^{-10}	88.0	8.8×10^{11}
Sal C 32	1.6×10^{6}	10^{-8}	26.0	2.6×10^{10}	10^{-9}	92.0	9.2×10^{10}	10^{10}	94.0	9.4×10^{11}

Table 2. Solving equations of bacteriophage kinetic titration in lysing bacterial host.

Salmonella isolates OD $_{600nm}$ = 1.0	**Initial amount (cell/ml)**	**Bacteriophage 1st infection**			**Bacteriophage 2nd infection**		
		12 h OD$_{600\ nm}$	**Phage ml^{-1}**	***Salmonella*** **(cell/ml)**	**12 h OD$_{600\ nm}$**	**Phage ml^{-1}**	***Salmonella*** **(cell/ml)**
S. typhi 16	$1.6 \times 10^{+6}$	0.40	$1.2 \times 10^{+8}$	$6.4\times^{+5}$	0.20	$3.31 \times 10^{+10}$	$1.3\times^{+5}$
S. typhi 32	$2.8 \times 10^{+6}$	0.36	$1.4 \times 10^{+8}$	$1.0\times^{+6}$	0.15	$3.72 \times 10^{+10}$	$1.5\times^{+5}$
S.7 16	$1.7 \times 10^{+6}$	0.38	$9.5 \times 10^{+8}$	$6.4\times^{+5}$	0.33	$4.14 \times 10^{+10}$	$2.1\times^{+5}$
S.7 32	$1.1 \times 10^{+6}$	0.42	$1.23 \times 10^{+9}$	$4.7\times^{+5}$	0.36	$4.55 \times 10^{+10}$	$1.7\times^{+5}$
Dr11 16	$0.9 \times 10^{+6}$	0.48	$1.65 \times 10^{+9}$	$4.3\times^{+5}$	0.42	$4.97 \times 10^{+10}$	$1.8\times^{+5}$
Dr11 32	$1.3 \times 10^{+6}$	0.54	$2.06 \times 10^{+9}$	$7.0\times^{+5}$	0.49	$5.38 \times 10^{+10}$	$3.4\times^{+5}$
Sal C 16	$1.5 \times 10^{+6}$	0.36	$2.48 \times 10^{+9}$	$5.4\times^{+5}$	0.55	$5.80 \times 10^{+10}$	$3.0\times^{+5}$
Sal C 32	$1.6 \times 10^{+6}$	0.44	$4.43 \times 10^{+9}$	$7.0\times^{+5}$	0.60	$6.32 \times 10^{+10}$	$4.2\times^{+5}$

$$\frac{dA}{dt} = -(ki.A.B - kd.AB) \quad (3)$$

$$\frac{d[AB]}{dt} = ki.[A].[B] - kd.[AB] \quad (4)$$

$$\boldsymbol{R} = R^{1a} + R^{0} + R^{1} + [drift(t - t_0)] \quad (5)$$

In the numerical kinetics equation, each replicated titer individually started from the *Salmonella* initial amount, and the total response calculated (Equations 1 to 5). The equations also contain terms for bacteria mass transport from initial amount of bacterial host to the first and second infection by phage, drift and time refractive index intervals.

To determine the kinetics lysis of bacteriophage efficancy and bacterial host cells decay rates, the lysis rates of *Salmonella* initial amounts were plotted exponentially against the phage potentiality in lysing bacteria. Furthermore, the decay profiles varied for each sample as shown in Table 2. While the viability of the phage decreased in a trend consistent with first infection decay kinetics, the bacteria displayed degradation patterns depending on incubation period before entering a second phase of infection that increased rates of lysing.

Table 3. Reducing absorbency of extracted virolysins OD/h.

Tested sample OD $_{600nm}$=1.0	Virolysins decay/h OD $_{600nm}$ <1.0
S. typhi 16	0.75
S. typhi 32	0.98
S.7 16	0.80
S.7 32	0.79
Dr11 16	0.92
Dr11 32	0.81
Sal C 16	0.85
Sal C 32	0.69

Solving bacteriophage exponential lysing rate; 1st infection [$y = 702302e^{-0.027x}$, 2nd infection $y = 107473e^{0.1582x}$] and their Spearman's rank correlation coefficient (R^2) = 0.06 and 0.8. The exponent positive integer corresponds to the repeat multiplication of the base (bacteria) and (e^{+bx}) with positive integer indicates the bacteria exponential decay and multiplication of phage in 12 h of incubation period.

Virolysins potentiality in lysing bacteria

Virolysin acts on *S. typhi* peptidoglycan, which has been used as a substrate to form the framework of cell wall hydrolysis. The enzyme activity and concentration were performed by turbidimetric measurement of the lysis under standardized conditions. The ability of the extracted phages' enzymes to lyse the *S. typhi* isolates was detected using Benedict's reagent; each at 16 and 32 µg/ml of ciprofloxacin was determined by measuring its optical densities at 600_{nm} as shown in Table 3.

The *S. typhi* lysis rate was determined as the reduction of OD_{600nm} by the active enzyme in the absence of bacteriophage particles and incubation time of 12 to 4 h.

The lytic potentialities of the virolysins and their release in the phage lytic cycle suggested that they are responsible for bacteria cell wall degradation and peptidoglycan hydrolysis. The estimated mechanisms of enzyme lysing rates of bacteria were based on determinations of the reaction velocity constants V/min calculated from the equation (Equations 6 to 11):

$$V = \frac{\Delta E}{t} ln \frac{C_0}{C_0 - C_t} \quad (6)$$

where $C_{0>0}\ and\ C_0 - c_t \neq 0$; in which V = the velocity of the reaction, ΔE = distance displacement, C_0= the initial concentration of *S. typhi* ml^{-1} (10^6 cell/ml at OD_{600nm}), C_t=final concentration of *S. typhi* ml^{-1} lysed at any given time interval = t.

Virolysins exponential kinetics

Enzyme kinetics are usually described by Michaelis-Menten equation (Bezerra et al., 2016), where the time-dependent decrease of substrate ($-\frac{dx}{dt}$) is a hyperbolic function of maximal velocity (V_{max}). If x = t is time and y = f (t) is the displacement (function) of a moving object, then:

$$\frac{dy}{dx} = f\ (V_{max}) \quad (7)$$

where f_0 (t) is the velocity (function). Thus f_0 (t_0) = 0 means that the velocity at time t_0 is 0, that is, the object is stationary at that moment.

$$\frac{dy}{dx} = f\ [\frac{\Delta E}{t}\ ln \frac{C_0}{C_0 - C_t}] \quad (8)$$

The substrate is catalyzed and the time-dependent decrease ($-\frac{dx}{dt}$) is a function of the quantity of the complex (C) at time (t):

$$\frac{dy}{dx} = \frac{d[\frac{\Delta E}{t}\ ln \frac{C_0}{C_0 - C_t}]}{dx} = -\frac{dx}{dt} = \lambda x \quad (9)$$

Kinetics exponential decay rate

The rate of the exponential decay can be measured by the ''recession of reaction velocity constants'' V, which has dimensions of V/time.

$$V = (\frac{dy}{dt} = -\lambda x) \quad (10)$$

where $x = -\frac{ty}{\lambda}, d \neq 0\ and\ \lambda \neq 0$ and solved by

$$[Y_t = y_0 e^{-bx}] \quad (11)$$

Graphically, V is the slope of the recession hydrograph on exponential axes tending to (0) and t is its reciprocal that solves the exponential decay in 4 h (Figure 3). Lysing of *S. typhi* using lytic enzymes showed irreversible interaction in 4 h, the initial optical density of tested samples was ($OD_{600\ nm}$< 1.0) when λ > 0 and the b is between 0 and 1. Solving the data on the double reciprocal plot showed that bacteria are decaying when each time x is increased, y decreased exponentially as shown in Figure 4.

The virolysins kinetics data that fit the exponential decay rate of *S. typhi* was given by negative exponential decay equation ($Y = ye^{-bx}$), with negative integer.

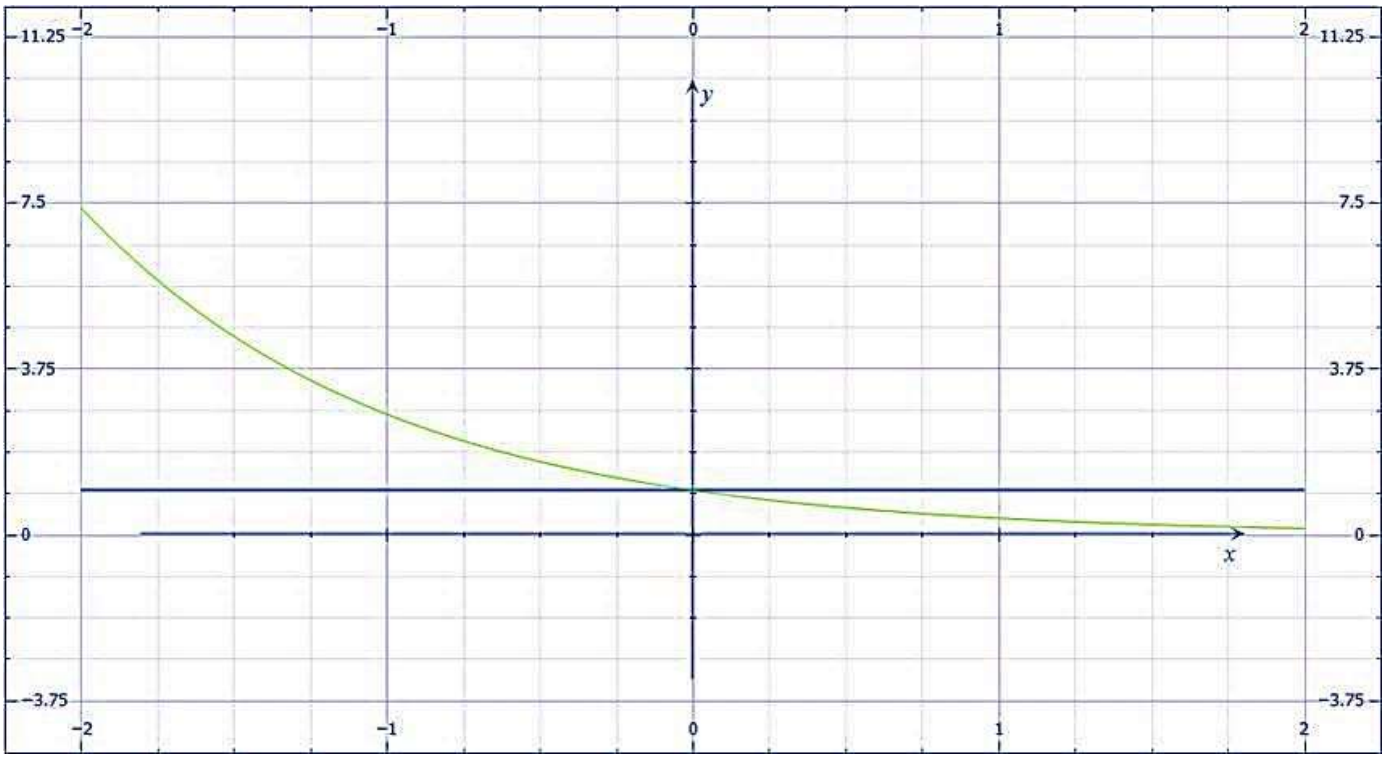

Figure 3. Virolysins kinetics exponential decay. Where V is the kinetics velocity, λ (lambda) is a positive rate termed the exponential decay constant, (Y_t) is the quantity at time t, and (y_0) is the initial absorbance = 1.0 at OD $_{600nm}$.

Table 4. The exponential decay rate of virolysins.

Sample	Exponential decay rate	coefficient
S. typhi 16	$y = 1.0262e^{-0.018x}$	$R^2 = 0.988$
S. typhi 32	$y = 1.0017e^{-0.001x}$	$R^2 = 0.954$
S.7 16	$y = 1.0192e^{-0.014x}$	$R^2 = 0.995$
S.7 32	$y = 1.0207e^{-0.014x}$	$R^2 = 0.988$
Dr11 16	$y = 1.0064e^{-0.005x}$	$R^2 = 0.997$
Dr11 32	$y = 1.0173e^{-0.014x}$	$R^2 = 0.999$
Sal C 16	$y = 1.0135e^{-0.01x}$	$R^2 = 0.991$
Sal C 32	$y = 1.0352e^{-0.025x}$	$R^2 = 0.997$

Coefficient $R^2 = 0.9$ is a very high value, and enzyme activity of the samples has a significant value ($P < 0.01$) which also indicates strong correlation of the reactions. If $b > 0$, we have exponential growth; if $b < 0$ exponential decay, b as actual rate can also be interpreted as the difference between an underlying growth rate and an underlying decay rate as shown in Table 4.

DISCUSSION

Enteric or typhoid fever is still a significant public health issue all over the world. It is a dangerous disease because of its long course and associated complications unless it is diagnosed early and treated (Effa et al., 2011). There are reports of changing clinical features in typhoid fever caused by multi-drug resistant *S. typhi.* This agrees with the susceptibility patterns of isolates' resistance that the present study revealed. However, drug resistance in typhoid fever is considered as one of the most important factors in the morbidity and mortality of the disease (Jain and Das Chugh, 2013). Therefore, bacteriophage therapy is one of the best antimicrobial alternative against resistant *S. typhi* due to its different mechanisms of action in lysing bacteria (Albino et al., 2014). The bacteriophages were specific, generally lysing

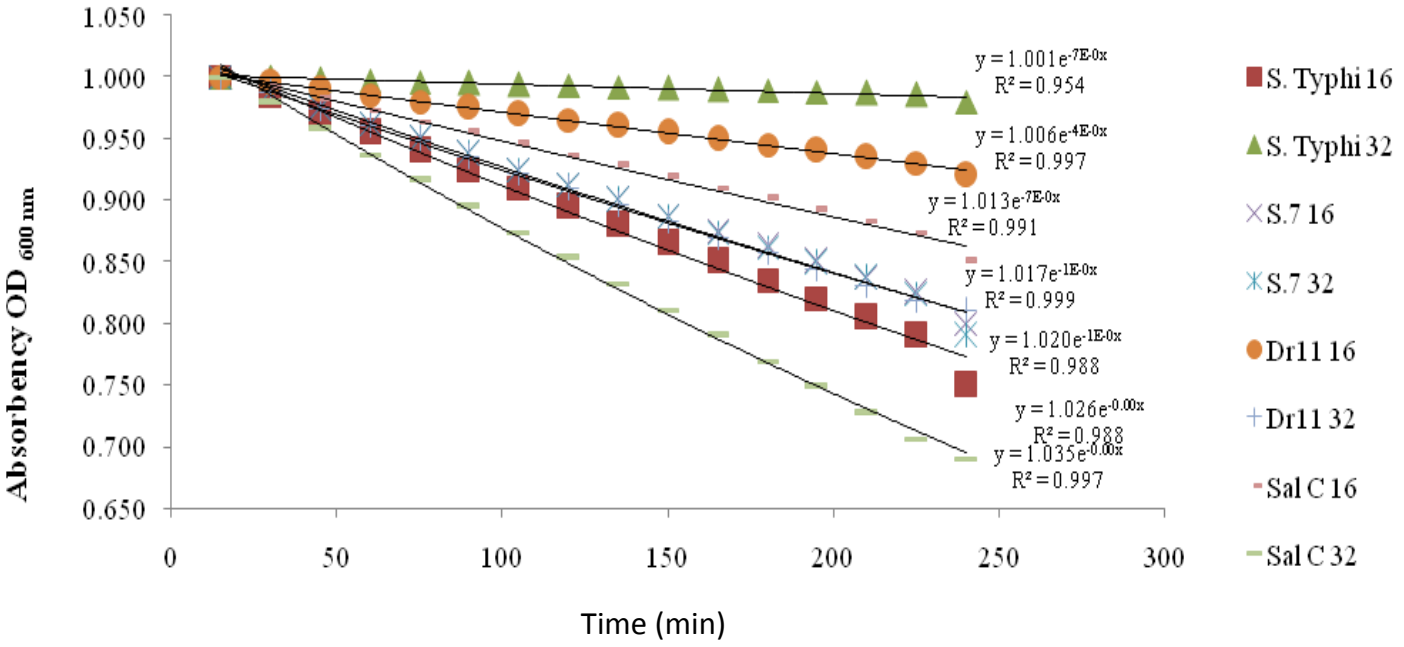

Figure 4. Virolysins kinetics exponential decay.

only the hosts on which they were isolated; the lysing rate and/or titeration kinetics are essential in bacteria decay measurements (Aviram and Rabinovitch, 2014). Consequently, it is required to isolate and characterize the infectious bacterium. Then, it can be matched with an effective lytic phage before treating using the multiplicity of infection [MOI] for bacteriophage amplification. This is in line with Chan and Abedon (2012) and Sillankorva et al. (2012), who stated that, the infection cycle utilized by a phage is an important phonemonon when choosing a phage for antibacterial application.

Another innovative approach of phage therapy is the utlization of phages' lytic enzymes namely virolysins instead of the whole virus, which can be generated via a targeted bacterium. Screening of phages-host interaction to increase lysis rates precisely (the kinetics exponential decay rate) with a functional lytic enzyme during phage infecting bacterial cells causes bacteriolysis and results in dead but intact bacterial cells (Filatova et al., 2015; Sun et al., 2015). Virolysins lysed cell wall peptidoglycan that yielded to primary amino sugars released and free intracellular components from hydrolyzed bacteria in the reaction qualitatively and quantitatively (Kadurugamuwa et al., 1998; Li et al., 2000). The capability of virolysins in lysing *S. typhi* can be induced in the absence of bacteriophage due to expression of functions from cell wall degraded by the enzyme (Clement et al., 1990; Sanz-Gaitero et al., 2013). Better results were obtained when phages and virolysins were mixed with bacterial cells in the solution because they adsorbed cell surfaces and cleaved to bonds, eventually causing lysis (Nelson et al., 2001; Busk and Lange, 2015).

Solving the kinetics equations by plotting data on sensorgram for bacteriophage decay and the double reciprocal for the enzyme activity support the *in vitro* reactions where lysis rate is constant meaning for exponentially distributed latent period of phage and bacterial cultures over incubation period (Precious and Barrett, 1993; Shinozaki-Kuwahara et al., 2001; Fong et al., 2002; Karthik et al., 2014). Lysing activity corresponding to an exponential descent in optical density (OD_{600}) was calculated to identify the area of each curve. The maximal determination coefficient (R^2) was calculated for an increasing sample size (n= number of measurements in time). This maximized R^2-value ensures the most reliable fit and hence the most reliable exponential regression. The slope of the curves was used to calculate the decrease in OD_{600} per unit of titer dilution at a certain time. The activity was calculated based on the amount of lytic enzymes added to a volume of 1 ml of cell suspension (Marova and Kovar, 1993; Cheng et al., 1994). The difference of exponential decay rate between bacteriophage and their extracted enzyme was mathematically approved by the occurrence of positive (e^{+bx}) and negative (e^{-bx}) exponent integers in the solved equations. This indicates multiplication and mortality of living organisms. The negative exponent integer described the population decay. It makes sense to define the exponential number raised to a negative integer exponent as decreasing of living bacteria and absence of

phages. Therefore, no resistant bacteria occurred after enzyme lysing and the susceptibility was 100% after 4 h of incubation period. As for antibiotics, bacteria have been reported to develop resistance against phage infection. A significant point with phage resistance is that it is associated with reduced bacterial virulence using enzybiotics; it is a great value to prevent phage resistance and have safe manipulation (Laanto et al., 2012).

Conclusion

Bacteriophage therapy and phage enzybiotics have been proven as effective agents for the elimination of a wide range of infectious bacteria including antibiotic resistant strains. Bacteriophage therapy showed lytic multiplication in their bacterial host. The lytic enzymes showed irreversible relationship of host decay in the absence of phage. Lytic enzymes are safe and time saving in the *in vitro* treatment of antibiotics resistant strains of *S. typhi.*

CONFLICT OF INTERESTS

The authors have not declared any conflict of interests.

ACKNOWLEDGEMENT

This research was funded by the University of Khartoum under the supervision of Prof. EL-Hussien as a part of Dr. Ayman Elshayeb PhD project.

REFERENCES

Ahluwalia V, Garg N, Kumar B, Walia S, Sati OP (2012). Synthesis, antifungal activity and structure-activity relationships of vanillin oxime-N-O-alkanoates. Nat. Prod. Commun. 7:1635-1638.

Albino LA, Rostagno MH, Hungaro HM, Mendonca RC (2014). Isolation, characterization, and application of bacteriophages for Salmonella spp. biocontrol in pigs. Foodborne Pathog Dis. 11:602-609.

Aviram I, Rabinovitch A (2014). Bacteria and lytic phage coexistence in a chemostat with periodic nutrient supply. Bull Math. Biol. 76:225-244.

Bezerra RM, Pinto PA, Fraga I, Dias AA (2016). Enzyme inhibition studies by integrated Michaelis-Menten equation considering simultaneous presence of two inhibitors when one of them is a reaction product. Comput. Methods Programs Biomed. 125:2-7.

Borris LC, Petersen MB, Lassen MR (2001). Prevention of thrombosis in hip alloplasty. Ugeskr Laeger 163:934-935.

Bryan D, El-Shibiny A, Hobbs Z, Porter J, Kutter EM (2016). Bacteriophage T4 Infection of Stationary Phase *E. coli*: Life after Log from a Phage Perspective. Front. Microbiol. 7:1391.

Busk PK, Lange L (2015). Classification of fungal and bacterial lytic polysaccharide monooxygenases. BMC Genomics 16:368.

Buyuktimkin B, Saier MH (2015). Comparative genomic analyses of transport proteins encoded within the genomes of Leptospira species. Microb. Pathog. 88:52-64.

Buyuktimkin B, Saier MH (2016). Comparative analyses of transport proteins encoded within the genomes of Leptospira species. Microb. Pathog. 98:118-131.

Chan BK, Abedon ST (2012). Phage therapy pharmacology phage cocktails. Adv. Appl. Microbiol. 78:1-23.

Cheng X, Zhang X, Pflugrath JW, Studier FW (1994). The structure of bacteriophage T7 lysozyme, a zinc amidase and an inhibitor of T7 RNA polymerase. Proc. Natl. Acad. Sci. 91:4034-4038.

Clement MV, Haddad P, Soulie A, Guillet J, Sasportes M (1990). Involvement of granzyme B and perforin gene expression in the lytic potential of human natural killer cells. Nouv. Rev. Fr. Hematol. 32:349-352.

Clinical and Laboratory Standards Institute (CLSI) (2012). Performance Standards for Antimicrobial Disk Susceptibility Tests. Approved Standard 32.

Courchesne NM, Parisien A, Lan CQ (2009). Production and application of bacteriophage and bacteriophage-encoded lysins. Recent Pat. Biotechnol. 3:37-45.

Effa EE, Lassi ZS, Critchley JA, Garner P, Sinclair D, Olliaro PL, Bhutta ZA (2011). Fluoroquinolones for treating typhoid and paratyphoid fever (enteric fever). Cochrane Database Syst. Rev. CD004530.

Feasey NA, Masesa C, Jassi C, Faragher EB, Mallewa J, Mallewa M, MacLennan CA, Msefula C, Heyderman RS, Gordon MA (2015). Three Epidemics of Invasive Multidrug-Resistant Salmonella Bloodstream Infection in Blantyre, Malawi, 1998-2014. Clin. Infect. Dis. 61(Suppl 4):S363-371.

Filatova LY, Donovan DM, Foster-Frey J, Pugachev VG, Dmitrieva NF, Chubar TA, Klyachko NL, Kabanov AV (2015). Bacteriophage phi11 lysin: Physicochemical characterization and comparison with phage phi80alpha lysin. Enzyme Microb. Technol. 73-74:51-58.

Fong CC, Lai WP, Leung YC, Lo SC, Wong MS, Yang M (2002). Study of substrate-enzyme interaction between immobilized pyridoxamine and recombinant porcine pyridoxal kinase using surface plasmon resonance biosensor. Biochim Biophys. Acta 1596:95-107.

Groman NB, Suzuki G (1963). Quantitative study of endolysin synthesis during reproduction of lambda phages. J. Bacteriol. 86:187-194.

Gupta V, Kaur J, Chander J (2009). An increase in enteric fever cases due to Salmonella Paratyphi A in & around Chandigarh. Indian J. Med. Res. 129:95-98.

Jain S, Das Chugh T (2013). Antimicrobial resistance among blood culture isolates of *Salmonella enterica* in New Delhi. J. Infect. Dev. Ctries 7:788-795.

Jones C, Darton TC, Pollard AJ (2014). Why the development of effective typhoid control measures requires the use of human challenge studies. Front Microbiol. 5:707.

Kadurugamuwa JL, Mayer A, Messner P, Sara M, Sleytr UB, Beveridge TJ (1998). S-layered Aneurinibacillus and Bacillus spp. are susceptible to the lytic action of *Pseudomonas aeruginosa* membrane vesicles. J. Bacteriol. 180:2306-2311.

Karthik L, Kumar G, Keswani T, Bhattacharyya A, Chandar SS, Bhaskara Rao KV (2014). Protease inhibitors from marine actinobacteria as a potential source for antimalarial compound. PLoS One 9:e90972.

Laanto E, Bamford JK, Laakso J, Sundberg LR (2012). Phage-driven loss of virulence in a fish pathogenic bacterium. PLoS One 7:e53157.

Li S, Norioka S, Sakiyama F (2000). Purification, characterization, and primary structure of a novel cell wall hydrolytic amidase, CwhA, from *Achromobacter lyticus*. J. Biochem. 127:1033-1039.

Lopez-Cuevas O, Castro-Del Campo N, Leon-Felix J, Gonzalez-Robles A & Chaidez C (2011). Characterization of bacteriophages with a lytic effect on various Salmonella serotypes and *Escherichia coli* O157:H7. Can. J. Microbiol. 57:1042-1051.

Madhulika U, Harish BN, Parija SC (2004). Current pattern in antimicrobial susceptibility of Salmonella Typhi isolates in Pondicherry. Indian J. Med. Res. 120:111-114.

Mainar-Jaime RC, Andres S, Vico JP, San Roman B, Garrido V, Grillo MJ (2013). Sensitivity of the ISO 6579:2002/Amd 1:2007 standard method for detection of Salmonella spp. on mesenteric lymph nodes from slaughter pigs. J. Clin. Microbiol. 51:89-94.

Marova I, Kovar J (1993). Spectrophotometric detection of bacteriolytic activity of diluted lysostaphin solutions. Folia Microbiol. 38:153-158.

Maszewska A (2015). Phage associated polysaccharide depolymerases - characteristics and application. Postepy higieny i medycyny doswiadczalnej, 69:690-702.
Meaney CA, Cartman ST, McClure PJ, Minton NP (2015). Optimal spore germination in Clostridium botulinum ATCC 3502 requires the presence of functional copies of SleB and YpeB, but not CwlJ. Anaerobe 34: 86-93.
Mooijman KA, Bahar M, Contreras N, Havelaar AH (2001). Optimisation of the ISO-method on enumeration of somatic coliphages (draft ISO 10705-2). Water Sci. Technol. 43:205-208.
Narasimhan S, Lee JW, Cheung RK, Gelfand EW, Schachter H (1988). Beta-1,4-mannosyl-glycoprotein beta-1,4-N-acetylglucosaminyltransferase III activity in human B and T lymphocyte lines and in tonsillar B and T lymphocytes. Biochem. Cell Biol. 66: 889-900.
Nelson D, Loomis L, Fischetti VA (2001). Prevention and elimination of upper respiratory colonization of mice by group A streptococci by using a bacteriophage lytic enzyme. Proc. Natl. Acad. Sci. 98: 4107-4112.
Patel J, Sharma M, Millner P, Calaway T, Singh M (2011). Inactivation of Escherichia coli O157:H7 attached to spinach harvester blade using bacteriophage. Foodborne Pathog. Dis. 8: 541-546.
Ploss M, Kuhn A (2010). Kinetics of filamentous phage assembly. Phys. Biol. 7:045002.
Precious WY, Barrett J (1993). Quantification of the control of carbohydrate catabolism in the tapeworm *Hymenolepis diminuta.* Biochem. Cell Biol. 71:315-323.
Salazar O, Asenjo JA (2007). Enzymatic lysis of microbial cells. Biotechnol. Lett. 29:985-994.
Sanz-Gaitero M, Keary R, Garcia-Doval C, Coffey A, van Raaij MJ (2013). Crystallization of the CHAP domain of the endolysin from Staphylococcus aureus bacteriophage K. Acta Crystallogr Sect. F. Struct. Biol. Cryst. Commun. 69:1393-1396.
Savary BJ, Hicks KB, O'Connor JV (2001). Hexose oxidase from Chondrus crispus: improved purification using perfusion chromatography(*). Enzyme Microb. Technol. 29:42-51.
Shinozaki-Kuwahara N, Hayakawa M, Shiroza T, Abiko Y, Fukushima K (2001). Purification and characterization of an oligo-isomaltosaccharide synthase from a Streptococcus sobrinus glucosyltransferase-I deficient mutant. Biosci. Biotechnol. Biochem. 65:1290-1295.
Sillankorva SM, Oliveira H & Azeredo J (2012). Bacteriophages and their role in food safety. Int. J. Microbiol. 2012:863945.
Skariyachan S, Prasanna A, Manjunath SP, Karanth SS, Nazre A (2016). Exploring the Medicinal Potential of the Fruit Bodies of Oyster Mushroom, Pleurotus ostreatus (Agaricomycetes), against Multidrug-Resistant Bacterial Isolates. Int. J. Med. Mushrooms 18:245-252.
Sun FF, Hong J, Hu J, Saddler JN, Fang X, Zhang Z, Shen S (2015). Accessory enzymes influence cellulase hydrolysis of the model substrate and the realistic lignocellulosic biomass. Enzyme Microb. Technol. 79-80:42-48.
Weill FX (2010). Typhoid fever: facing the challenge of resistant strains. Med Sci. (Paris) 26:969-975.
Yang H, Yu J, Wei H (2014). Engineered bacteriophage lysins as novel anti-infectives. Front Microbiol. 5:542.

African Journal of Biotechnology

Related Journals Published by Academic Journals

- *Biotechnology and Molecular Biology Reviews*
- *African Journal of Microbiology Research*
- *African Journal of Biochemistry Research*
- *African Journal of Environmental Science and Technology*
- *African Journal of Food Science*
- *African Journal of Plant Science*
- *Journal of Bioinformatics and Sequence Analysis*
- *International Journal of Biodiversity and Conservation*

academicJournals